

NAVAL POSTGRADUATE SCHOOL

Monterey, California



THESIS

H85793

DEVELOPMENT, QUALIFICATION AND
MEASUREMENTS IN TWO CURVED CHANNELS
WITH 40 TO 1 ASPECT RATIO

by

Randy E. Hughes

September 1989

Thesis Advisor
Co-Advisor

Phillip M. Ligrani
Chelakara S. Subramanian

Approved for public release; distribution is unlimited.

T247265

REPORT DOCUMENTATION PAGE

a Report Security Classification Unclassified		1b Restrictive Markings	
a Security Classification Authority		3 Distribution Availability of Report	
b Declassification Downgrading Schedule		Approved for public release; distribution is unlimited.	
Performing Organization Report Number(s)		5 Monitoring Organization Report Number(s)	
a Name of Performing Organization Naval Postgraduate School	6b Office Symbol (If applicable) 34	7a Name of Monitoring Organization Naval Postgraduate School	
c Address (city, state, and ZIP code) Monterey, CA 93943-5000		7b Address (city, state, and ZIP code) Monterey, CA 93943-5000	
a Name of Funding Sponsoring Organization Propulsion Directorate	8b Office Symbol (If applicable)	9 Procurement Instrument Identification Number MIPR C-800019-F	
c Address Research & Technology Activity, AVSCON US Army Aviation NASA-Lewis Research Ctr. Cleveland, OH 45433		10 Source of Funding Numbers	
		Program Element No	Project No
		Task No	Work Unit Accession No
1 Title (include security classification) DEVELOPMENT, QUALIFICATION AND MEASUREMENTS IN TWO CURVED CHANNELS WITH 40 TO 1 ASPECT RATIO			
2 Personal Author(s) Randy E. Hughes			
3a Type of Report Master's Thesis	13b Time Covered From To	14 Date of Report (year, month, day) September 1989	15 Page Count 83
6 Supplementary Notation The views expressed in this thesis are those of the author and do not reflect the official policy or position of the Department of Defense or the U.S. Government.			
7 Cosati Codes		18 Subject Terms (continue on reverse if necessary and identify by block number)	
Field	Group	Dean Vortex, Curved Channel, Heat Transfer Channel	
9 Abstract (continue on reverse if necessary and identify by block number)			
<p>Studies were conducted in two channels with identical internal dimensions. Each channel has mild curvature, 40 to 1 aspect ratio, and a 1.27 cm by 50.08 cm rectangular cross section. One channel is used for flow visualization, and one channel is used for heat transfer measurements. As part of the study, assembly of the heat transfer channel was completed along with qualification tests of internal flow behavior.</p> <p>In the transparent channel, videos and still photographs were taken of visualized flow for Dean numbers from 60 to 200 and angular positions from 85 degrees to 175 degrees from the start of curvature. These data provide new information on the unsteady behavior of Dean vortex pairs, especially how vortex pairs merge and divide.</p> <p>Assembly of the heat transfer channel included installation of insulation to minimize conductive heat losses, completion of wiring of thermocouples used for surface temperature measurements, wiring of heater power supplies and controlling systems, and assembly of piping from the blower to the channel including installation of regulation valves and flow metering orifices. Velocity and pressure surveys were conducted downstream of the instrumented section. For Dean numbers from 60 to 158, these distributions were either spanwise uniform or spanwise periodic, as expected, providing qualification of internal behavior in the channel.</p>			
20 Distribution Availability of Abstract		21 Abstract Security Classification	
<input checked="" type="checkbox"/> unclassified unlimited <input type="checkbox"/> same as report <input type="checkbox"/> DTIC users		Unclassified	
22a Name of Responsible Individual		22b Telephone (Include Area code)	22c Office Symbol
Phillip M. Ligrani		(408) 646-3382	69Li

Approved for public release; distribution is unlimited.

Development, Qualification and
Measurements in Two Curved Channels
With 40 to 1 Aspect Ratio

by

Randy E. Hughes
Lieutenant, United States Navy
B.S.M.E., Purdue University, 1981

Submitted in partial fulfillment of the
requirements for the degree of

MASTER OF SCIENCE IN MECHANICAL ENGINEERING

from the

NAVAL POSTGRADUATE SCHOOL
September 1989

ABSTRACT

Studies were conducted in two channels with identical internal dimensions. Each channel has mild curvature, 40 to 1 aspect ratio, and a 1.27 cm by 50.08 cm rectangular cross section. One channel is used for flow visualization, and one channel is used for heat transfer measurements. As part of the study, assembly of the heat transfer channel was completed along with qualification tests of internal flow behavior.

In the transparent channel, videos and still photographs were taken of visualized flow for Dean numbers from 60 to 200 and angular positions from 85 degrees to 175 degrees from the start of curvature. These data provide new information on the unsteady behavior of Dean vortex pairs, especially how vortex pairs merge and divide.

Assembly of the heat transfer channel included installation of insulation to minimize conductive heat losses, completion of wiring of thermocouples used for surface temperature measurements, wiring of heater power supplies and controlling systems, and assembly of piping from the blower to the channel including installation of regulation valves and flow metering orifices. Velocity and pressure surveys were conducted downstream of the instrumented section. For Dean numbers from 50 to 158, these distributions were either spanwise uniform or spanwise periodic, as expected, providing qualification of internal behavior in the channel.

1 RISK
#85793
C.1

TABLE OF CONTENTS

I. INTRODUCTION	1
II. EXPERIMENTAL FACILITIES	2
A. CURVED CHANNELS	2
1. Curved Channel for Heat Transfer Studies	2
2. Blower	3
3. Orifice Plate Assembly and Flow Rate Measurement	4
4. Heaters	5
5. Thermocouple Placement	6
6. Temperature Measurement	6
7. Insulation	7
8. Data Acquisition System for Temperature Measurement	7
9. Data Acquisition System for Mixed Mean Temperature Measurement ..	7
10. Heater System Wiring	9
III. RESULTS	10
A. FLOW VISUALIZATION EXPERIMENTAL PROCEDURE	10
B. FLOW VISUALIZATION IN A CURVED CHANNEL	10
C. VELOCITY AND PRESSURE SURVEYS	12
IV. SUMMARY AND CONCLUSIONS	13
LIST OF REFERENCES	71
INITIAL DISTRIBUTION LIST	72

LIST OF TABLES

Table 1.	THERMOCOUPLE LOCATIONS	14
Table 2.	THERMOCOUPLE LOCATIONS (CONTINUED)	15
Table 3.	THERMOCOUPLE LOCATIONS (CONTINUED)	16
Table 4.	THERMOCOUPLE LOCATIONS (CONTINUED)	17

LIST OF FIGURES

Figure 1.	Transparent Channel	18
Figure 2.	Smoke Generator	19
Figure 3.	Heat Transfer Channel Rear Quarter View	20
Figure 4.	Heat Transfer Channel Inlet	21
Figure 5.	Arrangement drawing of blower, plenum #1 and #2, orifice and globe valve.	22
Figure 6.	Heat Transfer Channel Front Quarter View	23
Figure 7.	Orifice Plate Assembly Details	24
Figure 8.	Heat Transfer Channel Thermocouple Installation	25
Figure 9.	Heat Transfer channel Heater Identification	26
Figure 10.	Concave Heater Thermocouple Placement	27
Figure 11.	Convex Heater Thermocouple Placement	28
Figure 12.	Heat Transfer Channel Insulation Drawing	29
Figure 13.	Heat Transfer Channel Insulation Photograph	30
Figure 14.	Heat Transfer Channel Data Acquisition System for Temperature Measurement	31
Figure 15.	Heat Transfer Channel Data Acquisition System for Flow Measurement	32
Figure 16.	Traversing Mechanism	33
Figure 17.	Heater and Control Circuit Wiring Diagram	34
Figure 18.	Heat Transfer Channel Heater Control Variacs	35
Figure 19.	Operator Station	36
Figure 20.	Flow Visualization Results $De = 75 \theta = 85^\circ$	37
Figure 21.	Flow Visualization Results $De = 75 \theta = 95^\circ$	38
Figure 22.	Flow Visualization Results $De = 75 \theta = 135^\circ$ (1 of 10)	39
Figure 23.	Flow Visualization Results $De = 75 \theta = 135^\circ$ (2 of 10)	40
Figure 24.	Flow Visualization Results $De = 75 \theta = 135^\circ$ (3 of 10)	41
Figure 25.	Flow Visualization Results $De = 75 \theta = 135^\circ$ (4 of 10)	42
Figure 26.	Flow Visualization Results $De = 75 \theta = 135^\circ$ (5 of 10)	43
Figure 27.	Flow Visualization Results $De = 75 \theta = 135^\circ$ (6 of 10)	44
Figure 28.	Flow Visualization Results $De = 75 \theta = 135^\circ$ (7 of 10)	45
Figure 29.	Flow Visualization Results $De = 75 \theta = 135^\circ$ (8 of 10)	46

Figure 30. Flow Visualization Results $De = 75$ $\theta = 135^\circ$ (9 of 10)	47
Figure 31. Flow Visualization Results $De = 75$ $\theta = 135^\circ$ (10 of 10)	48
Figure 32. Flow Visualization Results $De = 100$ $\theta = 95^\circ$	49
Figure 33. Flow Visualization Results $De = 100$ $\theta = 105^\circ$	50
Figure 34. Flow Visualization Results $De = 100$ $\theta = 145^\circ$	51
Figure 35. Flow Visualization Results $De = 100$ $\theta = 155^\circ$	52
Figure 36. Flow Visualization Results $De = 125$ $\theta = 115^\circ$ (1 of 2)	53
Figure 37. Flow Visualization Results $De = 125$ $\theta = 115^\circ$ (2 of 2)	54
Figure 38. Flow Visualization Results $De = 100$ $\theta = 125^\circ$ (1 of 2)	55
Figure 39. Flow Visualization Results $De = 100$ $\theta = 125^\circ$ (2 of 2)	56
Figure 40. Flow Visualization Results $De = 100$ $\theta = 125^\circ$ (1 of 2)	57
Figure 41. Flow Visualization Results $De = 100$ $\theta = 125^\circ$ (2 of 2)	58
Figure 42. Flow Visualization Results $De = 75$ $\theta = 135^\circ$ (1 of 2)	59
Figure 43. Flow Visualization Results $De = 75$ $\theta = 135^\circ$ (2 of 2)	60
Figure 44. Flow Visualization Results $De = 75$ $\theta = 135^\circ$ (1 of 2)	61
Figure 45. Flow Visualization Results $De = 75$ $\theta = 135^\circ$ (2 of 2)	62
Figure 46. Streamwise Velocity Contours in a Curved Channel, $De = 50$	63
Figure 47. Streamwise Velocity Contours in a Curved Channel, $De = 75$	64
Figure 48. Streamwise Velocity Contours in a Curved Channel, $De = 100$	65
Figure 49. Streamwise Velocity Contours in a Curved Channel, $De = 150$	66
Figure 50. Total Pressure Contours in a Curved Channel, $De = 50$	67
Figure 51. Total Pressure Contours in a Curved Channel, $De = 75$	68
Figure 52. Total Pressure Contours in a Curved Channel, $De = 100$	69
Figure 53. Total Pressure Contours in a Curved Channel, $De = 155.55$	70

LIST OF SYMBOLS

A	Area
d	Channel Height
D_e	Dean Number
K	Flow Coefficient
m	Mass Flowrate
ΔP	Pressure Drop
r	Channel Radius
Re	Reynolds Number
ρ	Density
t	Local Mean Temperature
T	Temperature
u	Local Mean Streamwise Velocity
U	Bulk Velocity
V	Voltage
Y	Expansion Coefficient

Subscripts:

ch	Channel
i	Inner
m	Mixed Mean
OR	Orifice Plate
p	Pipe

ACKNOWLEDGEMENTS

I should like to express my sincere gratitude to Professor Phillip M. Ligrani for his expert guidance, advice and patience which were instrumental in the completion of this study. I should also like to thank Professor Chelakara S. Subramanian for his astute software writing abilities.

Finally, to my beautiful wife, Terry, whose steadfast love and support made the completion of this work a reality, thank you.

I. INTRODUCTION

Centrifugal instabilities are important in the development of flows over concave surfaces which occur on the pressure side of turbine blades and airfoils. The primary consequence of centrifugal instabilities is the development of pairs of counter rotating vortices. In boundary layer flows over concave surfaces, these vortices are called Taylor-Gortler vortices. In curved channel flows layers, these vortices are called Dean vortices.

Previous flow visualization studies were performed by Baun, Siedband and Longest [Refs. 1,2,3] using the same channel as this study. Baun [Ref. 1] also performed a series of experiments using a subminiature crossed-wire probe to show the principle and harmonic frequencies for twisting Dean vortex flow for Dean numbers greater than 165. Siedband [Ref. 2] performed flow visualization studies using a smoke wire for a Dean number range of 167 to 461. Longest [Ref. 3] performed flow visualization studies for a Dean number of 75 and an angular position of 135° from the beginning of curvature in the transparent curved channel where he observed certain centrifugal instability patterns. Different instability patterns are expected to occur in other ranges of Dean numbers.

The objectives of the present study are to obtain additional flow visualization results for Dean numbers 75, 100 and 125 and angular positions of 85° to 155° in 10° increments from the beginning of curvature as they develop in a curved channel with mild curvature, 40 to 1 aspect ratio, a radius ratio of 0.979, and internal dimensions of 1.27 cm by 50.80 cm (.5 in. by 20 in.). Also of interest is the development of a facility to measure spanwise variations of surface heat transfer due to the presence of Dean vortex pairs.

Thesis organization is as follows. The experimental apparatus is discussed in Chapter II. The experimental procedure is discussed in Chapter III. Flow visualization and velocity and pressure results are given in Chapter IV. Chapter V gives a summary and conclusions. All figures referenced in the text of the thesis are found after Chapter V.

II. EXPERIMENTAL FACILITIES

A. CURVED CHANNELS

Two rectangular curved channels were used to obtain data. Figure 1 shows the transparent curved channel used for flow visualization studies. Figure 3 shows the second curved channel used for measurement of surface heat transfer distributions. Both channel interiors are dimensionally identical at 1.27 cm by 50.80 cm (.5 in. by 20 in.). The heat transfer channel is different from the transparent channel and unique in itself since it is designed to accommodate expansion due to heat input. Details of the construction and design of the transparent channel are contained in Siedband and Baun [Refs. 2,1].

On the heat transfer channel, the inlet and Plenum #1 rest on plexiglass skids to allow for longitudinal expansion during heating. Figure 12 shows how the convex and concave surfaces of the heat transfer channel rest on the sidewalls which are rigidly attached to the channel supports. This arrangement also allows for spanwise expansion of the convex and concave surfaces during heating.

1. Curved Channel for Heat Transfer Studies

The heat transfer channel is now discussed. Figure 4 shows a side view of the channel inlet. The flow inlet consists of a rectangular lip which is constructed of quarter circumference sections of 15.2 cm outside diameter plexiglass pipe. Flow then enters a 25.4 cm by 50.8 cm rectangular duct which houses an aluminum honeycomb and three screens stretched across the cross section. Distances between the honeycomb, following screen, and adjacent screens are about the same, approximately 10 cm. The honeycomb and screens reduce the spatial non-uniformities of the flow. A 20 to 1 contraction ratio nozzle connects the inlet to the duct.

The shape of the nozzle is given by a fifth order polynomial with respect to streamwise distance. The dimensions of the nozzle were selected to ensure that separation did not occur at its exit and to minimize the possibility of transition to turbulent flow. Two continuous pieces of lexan, each approximately 3 mm thick, are employed in the construction of the upper and lower surfaces of the inlet. Portions of these same pieces are used for the nozzle walls thereby eliminating a seam between the nozzle and the straight channel test section.

After the nozzle, flow enters the upper section of the curved duct. This portion of the duct is straight and has inside dimensions of 1.27 cm by 50.8 cm (.5 in. by 20 in.). The length of the straight section is 2.44 m and allows the flow to become fully developed in the Dean number ranges used before entering the 180 ° curved section. The convex wall in the curved section has a 59.69 cm radius of curvature. The concave wall has a 60.69 cm radius of curvature. Flow then enters another 2.44 m straight section, which is followed by a diffuser and outlet plenum. Figure 5 shows the arrangement of the upper and lower straight sections and the outlet plenum, Plenum #1.

A major difference between the transparent channel inlet and that of the heat transfer channel is in the mounting used to support the inlet. The transparent channel inlet is rigidly affixed to the support frame for the channel. The heat transfer channel inlet rests on two plexiglass skids that allow it to slide to account for longitudinal expansion of the upper portion of the channel during heating. Figure 5 shows the arrangement of the channel inlet and plenum number one.

2. Blower

An ICG Industries type 10P blower is used to depressurize Plenum # 2 below atmospheric pressure. Figure 5 shows that the blower is connected directly to Plenum #2. Air is drawn from Plenum #1 via a 5.08 cm inside diameter PVC pipe, globe valve, and 3.81 cm (1.5 in.) orifice plate. The blower produces 10.2 cm of water vacuum at 4.82 m^3/min volumetric flowrate. By varying the flowrate, Dean numbers from 20 to 220 can be produced in the channel. The flowrate is set using a globe valve and measured by means of a pressure drop across an orifice.

The suction side of the blower is connected to Plenum #2 via a vibration damper. The vibration damper is a thin sheet of plastic wrapped around the outlet of Plenum # 2 and the inlet of the blower. The plastic is attached to the plenum and the blower with pieces of double sided tape. Standard hose clamps were then placed over the outside and tightened to insure no leaks exist. A second vibration damper of the same type is placed between Plenum #2 and the orifice. Both of these vibration dampers are installed to isolate the curved channel from blower motor vibrations.

Figure 6 shows the actual arrangement of the blower, Plenum # 2, the vibration dampers, orifice, globe valve, and Plenum #1. The blower was positioned just below the tunnel inlet and between the upper and lower straight sections of the channel to maximize the compactness of the test facility.

3. Orifice Plate Assembly and Flow Rate Measurement

The flowrate through the heat transfer channel is determined from the pressure drop across a 3.81 cm (1.5 in.) standard ASME orifice. Figures 5 and 6 show the location of the orifice. Figure 7 shows orifice plate manufacturing and orientation details.

A pressure tap is located 1.9 cm (.75 in. or one half pipe diameter) upstream of the orifice plate, and a second tap is located 3.81 cm (1.5 in. or one pipe diameter) downstream of the orifice plate. A water manometer is used to measure the pressure drop between the tap locations, as the first step in determining the flowrate and Dean number. Details of this process are given by Siedband [Ref.2], but for completeness, a general description of the procedure is also given here.

Using the pressure drop across the orifice plate, the mass flowrate through the channel is determined using the following equation:

$$\dot{m} = KA_{OR}Y\sqrt{2\rho\Delta P}$$

Where:

$\dot{m} \equiv$ mass flowrate

$K \equiv$ flow coefficient (ASME tables)

$A_{OR} \equiv$ orifice area

$Y \equiv$ expansion coefficient

$\rho \equiv$ air density

$\Delta P \equiv$ pressure drop across orifice

Using the mass flowrate, \dot{m} , the pipe Reynolds number, Re_p , is determined using the equation given by:

$$Re_p = \frac{\dot{m}d_p}{\rho v A_p}$$

where:

$d_p \equiv$ pipe diameter

$v \equiv$ kinematic viscosity

$A_p \equiv$ pipe cross-sectional area

This iterative process is continued until the mass flowrate converges to within one percent for two successive calculations. The final value of the Dean number, D_e , is determined from the following equation:

$$D_e = \left[\frac{\dot{m}}{\rho A_{ch}} \right] \left[\frac{d}{v} \right] \sqrt{\frac{d}{r_i}}$$

where:

$A_{ch} \equiv$ channel area

$r_i \equiv$ inside radius of channel curvature

$d \equiv$ channel height

4. Heaters

Figure 9 shows a side view of the heat transfer channel including locations of the four heated sections. The flow enters through the inlet and contraction nozzle and then travels past the heaters and out of the channel as depicted by the flow arrows. The heaters on the outer surface of the channel are labeled Concave Heaters No. 1 and No. 2 (CC1 and CC2). Heated sections on the inside of the channel are labeled Convex Heaters No. 1 and No. 2 (CV1 and CV2). The number 1 denotes the first heaters encountered by the flow.

CC1 and CV1 heated sections are each instrumented with 15 thermocouples. Numbering is shown in Figures 10 and 11. The flow then travels through the curved section past CC2 and CV2. CC2 and CV2 heated sections are each instrumented with 85 thermocouples. Numbering is as shown in Figures 10 and 11.

Four custom made etched foil heaters manufactured by the Electrofilm Corporation are used in the construction of the heat transfer channel. Each heater provides uniform heat flux boundary conditions at the channel walls and has a 2 kw power capacity. The heater dimensions are 38.1 cm by 152.4 cm (15 in. by 60 in.). The leading edge of the CC1 and CV1 heaters is 91.4 cm downstream from the inlet. The heaters are attached to the convex and concave walls in the manner discussed by Schwartz [Ref.4].

Figure 8 shows the arrangement of the liners, thermocouples and heaters as they were assembled. Outside the lexan channel walls are four layers of .001 in. thick Sticky Back adhesive manufactured by the 3M Company. The heater is installed and held in place using 3M-467 transfer adhesive.

Amounts of conduction loss and contact resistance were determined by Bella [Ref. 5] using full scale models of both straight and curved heater sections. With insulation applied as described later in this chapter, conduction losses are less than three percent of the total power to the heaters. The thermal contact resistance between the thermocouple and surfaces exposed to the flow is $3.4 \times 10^{-3} \text{ m}^2 \text{ }^\circ\text{C/watt}$.

5. Thermocouple Placement

Within the coordinate system, X denotes the streamwise distance from the leading edge of CC1 and CV1, Z is measured from the spanwise centerline of the channel and Y is measured from the mid-plane between the two channel walls. The Thermocouple Location Table 1 gives the X and Z coordinates of each thermocouple.

Four thermocouples are used to measure ambient temperatures in the vicinity of the heat transfer channel and the mixed mean inlet and mixed mean outlet temperatures. One is located near the concave wall in the curved section of the channel and one is located near the convex wall. These measure ambient temperature. One is located in the channel inlet and one is used to traverse the measurement slot located 19 cm (7.5 in.) downstream from the test section. These measure channel mixed mean inlet temperature and mixed mean outlet temperature.

In the center portions of CC2 and CV2, fifteen thermocouples are spaced over a total distance of 3.81 cm (1.5 in.). This positioning is used to measure local wall temperatures as they are affected by the presence of Dean vortices. The spanwise spread of the thermocouples covers a distance equivalent to about one and one-half vortex pairs.

6. Temperature Measurement

Surface temperature measurements in the heat transfer channel, are obtained using 200 copper-constantan thermocouples. Thermocouples 1 to 30 are connected to data acquisition channels 0 to 29. Thermocouples 31 to 115 are connected to data acquisition channels 30 to 79 and 100 to 134. Thermocouples 116 to 200 are connected to data acquisition channels 135 to 179 and 200 to 239. The mixed mean inlet thermocouple, ambient convex thermocouple, ambient concave thermocouple and mixed mean outlet thermocouple are connected to data acquisition channels 240 to 243, respectively.

The voltage readings from the 200 heat transfer channel thermocouples, the mixed mean inlet thermocouple, mixed mean outlet thermocouple and the ambient concave thermocouple are converted to temperatures using the equation given by:

$$T = -1.988321 + 29436.53V - 2636568V^2 + 363932000V^3$$

The voltage readings from the ambient convex thermocouple are converted to temperature using the equation given by:

$$T = -1.816347 + 29287.91V - 2622880V^2 + 373752000V^3$$

Where:

$T \equiv$ temperature ($^{\circ}$ C)

$V \equiv$ thermocouple voltage (volt)

7. Insulation

Black foam insulation manufactured by the Halstead Company is used to minimize heat losses by conduction from the curved channel heat transfer section to the surrounding environment. Figure 12 shows how three different thicknesses of insulation are used to build four layers to give a total thickness of 7.0 cm (2.8 in.). The same thickness of insulation is applied to the exterior portions of all four heated sections. The first layer is 0.64 cm (.25 in.) thick and installed directly over the heaters between the lexan channel supports. The second layer is 1.27 cm (.50 in) thick, and also placed between the lexan supports. Third and fourth layers are each 2.54 cm (1.00 in.) thick, and secured in place by use of duct tape, as evident from the photographs in Figures 3 and 13.

8. Data Acquisition System for Temperature Measurement

Figure 14 shows the arrangement of the equipment used to obtain temperature data. Voltages from the copper-constantan thermocouples are read by Hewlett-Packard type T20 relay multiplexer card assemblies for the type T thermocouples. These assemblies contain thermocouple compensation to give voltages relative to 0 $^{\circ}$ C, and are installed in a 3497A Low Speed Data Acquisition/Control Unit or a 3498A extender. These units are controlled by a Hewlett-Packard 9836S computer. Custom designed software is used to direct and control the operation of the 3497A and 3498A as voltages from 204 thermocouples are read, processed and recorded.

9. Data Acquisition System for Mixed Mean Temperature Measurement

A check on heat transfer measurements is provided if the mixed mean temperature at the exit of the heated sections equals the mixed mean temperature determined

from the inlet mixed mean temperature and the net heat input. The mixed mean temperature at the exit of the heated sections is determined at a measurement slot located 19 cm (7.5 in.) downstream of the edge of the heated sections. Here, the mixed mean temperature is determined using the following equation:

$$t_m = \frac{1}{A_{ch} U} \int u t dA$$

Where:

$t_m \equiv$ mixed mean temperature

$A_{ch} \equiv$ channel area

$U \equiv$ bulk velocity (spacially averaged)

$u \equiv$ local mean streamwise velocity

$t \equiv$ local mean temperature

The mean temperature, t , is measured using the "mixed mean outlet thermocouple" mentioned earlier. This thermocouple is traversed using the same apparatus and procedures as for the pressure probes as described below.

The local mean streamwise velocity, u , is measured using a miniature five hole pressure probe described by Baun [Ref. 1]. Figure 15 shows the arrangement of the data acquisition system used during flow measurement. Five Validyne model DP103-06 variable reluctance pressure transducers are used with the probe to convert pressures into voltages by Celesco CD10D Carrier Demodulators. These units produce a DC output proportional to the pressure signal sent from the transducers. The DC output is then received by a Hewlett-Packard 3497A Low Speed Data Acquisition/Control unit with a 3498A extender. A Hewlett-Packard 9836S computer is used to control the data acquisition system, record the data, and index the pressure probes to the next position using a traversing mechanism. This two dimensional traversing device, used in conjunction with the traveling block shown in Figure 16, allows for spanwise and radial movement of the pressure probe. Signals to move the pressure probe are generated by the computer and sent to a model PMS085-C2AR Mitas Motion controller and a model PMS-D050 Mitas Motor Drive. Two separate signals from the motor drive direct the model M092-FD310 Superior Electric stepping motors to rotate drive screws and move

traveling blocks. This procedure is repeated to traverse a 5.08 cm (2 in.) spanwise distance and 1.02 cm (.4 in.) radial distance gathering 320 points of data in .127 cm (.05 in.) steps.

A miniature Kiel probe is also used to gather total pressure readings to further qualify flow behavior in the heat transfer channel and to check total pressure readings from the miniature five-hole probe. The diameters of the shield and pressure sensing port of the Kiel probe are 1.59 mm (.0625 in.) and .4mm (.0158 in.) respectively. A Celesco model LCVR variable reluctance differential pressure transducer was used in conjunction with the Kiel probe. All other procedures are the same as for the miniature five-hole probe.

10. Heater System Wiring

Each heater is powered by a separate variac connected to a wall outlet. Figure 17 shows heater circuits which include the variacs, where P denotes variable transformer (variac), S denotes shunt and H denotes heater. The variacs are Superior Electric type 136B devices. With these, voltages and currents are adjustable from 0 to 115 volts and 0 to 10 amps, respectively. Figure 18 shows a photograph of the variacs.

Electric current to each heater is monitored using 50 mv 10 amp shunt resistors. These are included in circuits wired to a switch which allows voltage drops across each shunt and each heater to be easily measured with the single digital volt-ohm meter shown in Figure 19. From these, power inputs to each heater are determined.

III. RESULTS

A. FLOW VISUALIZATION EXPERIMENTAL PROCEDURE

The procedures used to set up the transparent channel for flow visualization are now discussed.

Flow visualization techniques are discussed at length by Longest [Ref. 3], but are also briefly summarized here. After selecting and establishing the Dean number as described in the Experimental Facilities chapter, the smoke generator is energized. Figure 2 shows a drawing of the smoke generator. The channel blower reduces the inlet pressure to below atmospheric pressure allowing smoke to be ingested. When smoke is introduced into the channel inlet, the inlet is filled about half-way.

The outside of the convex wall is covered with a liner with spanwise slits cut at 10 ° increments from 0 ° to 185 ° angular positions. A General Radio Type 1531-A Strobatac strobe light, located at the center of curvature of the transparent channel, is positioned at the prescribed angular position and energized. Using a Sony DXC-3M video camera with a Fujinon TV-Z 1:1 7/10-140 mm DCL-914BY zoom lens, flow phenomena are recorded on Sony KCS20BR videocassettes. The orientation of the camera is at about a right angle to the strobe light source with the flow always moving away from the camera. Flow patterns at each Dean number and angular position are recorded for about one minute.

Still photographs are taken of a video monitor as it replays the videotape using a Nikon F-3 SLR camera with a 55 mm, f-2.8 lens. Kodak Tri-X 400 ASA film is used in this camera.

B. FLOW VISUALIZATION IN A CURVED CHANNEL

Flow visualization results for the 40 to 1 aspect ratio transparent curved channel are presented in Figures 20 through 45. The position of the observer is radially outside of the concave wall with the convex surface at the top of each photograph and the concave surface at the bottom. In each sequence of photographs, time increases from the top to the bottom with the flow direction being into the page. The dimensions of the observed phenomena are approximately 4.5 cm (1.5 in.) in the spanwise direction and 1.27 cm (.50 in.) in the radial direction.

Figures 20 and 21 show the flow visualization results for a Dean number of 75 and angular positions of 85 ° and 95 ° from the start of curvature, respectively. The time

interval between each photograph is $1/10$ of a second. Spanwise varying smoke patterns are evident in Figure 20. Here, there is no evidence of Dean vortex pairs since complete mushroom-shaped patterns are not present. In Figure 21, complete mushroom-shaped patterns indicate the presence of Dean vortex pairs. Spanwise shifting of the circular smoke patterns and Dean vortex pairs is apparent in both sets of photographs.

Figures 22 through 31 show photographic results for a Dean number of 75 and angular position of 135° . The time interval between photographs in these sequences is $1/30$ of a second. These results are discussed in detail by Longest [Ref. 3].

Figure 32 shows photographic results for a Dean number of 100 and an angular position of 95° . Here, the time interval between photographs is $1/10$ second. Fully formed Dean vortex pairs are evident with significant spanwise unsteadiness. A space appears between vortex pairs near the center, where new vortex pairs seem to develop. Afterwards, pairs seem to shift to equalize their spacing.

Figure 33 shows photographic results for a Dean number of 100 and an angular position of 105° . Here, the time interval between photographs is $1/10$ second. Significant unsteadiness and distortion are evident. In several cases, larger vortex pairs wrap one 'petal' around an adjacent smaller pair to eventually engulf it. This often allows space for new vortex pairs to grow.

Figure 34 shows photographic results for a Dean number of 100 and an angular position of 145° , where the time interval between photographs is $1/30$ of a second. Figure 35 shows photographic results for a Dean number of 100 and an angular position of 155° , where the time interval is $1/10$ of a second. For both sets, much activity is apparent including vortex pair growth, vortex pair expansion, spanwise shifting of pairs, and possibly some vortex pair division.

In figures 36 through 45, the time interval between photographs is $1/30$ of a second. Figures 36 and 37 shows photographic results for a Dean number of 125 and angular position 115° . Figure 36 shows clearly defined rocking motion evidencing twisting Dean vortex flow. This continues in Figure 37 which shows a smaller vortex pair being engulfed by a larger vortex pair.

Figures 38 through 41 show photographic results for a Dean number of 100 and angular position 125° from the start of curvature. Figures 38 and 39 show a large vortex pair engulfing a smaller vortex pair to its right. Figure 40 and 41 show how two vortex pairs can approach each other such that adjacent vortices cancel. A new pair is then evident which replaces the original two pairs.

Figures 42 through 45 show photographic evidence for Dean number 75 and angular position 135° . Here twisting Dean vortex flow is present with lower frequencies and smaller amplitudes of oscillation compared to results in Figure 36. This is shown by slight rocking of Dean vortex pairs.

C. VELOCITY AND PRESSURE SURVEYS

Figures 46 through 53 show time-averaged streamwise velocity and total pressure distributions measured in the heat transfer channel 19 cm (7.5 in.) downstream from the end of curvature. These data are given for Dean numbers from 50 to 150. The methods used to obtain this data are described by Ligrani, Singer and Baun [Ref. 6]. In each figure, the convex wall is at the top of the figure and the concave wall is at the bottom. Flow is into the page. The dimensions of the observed phenomena are 10.16 cm (4.0 in.) in the spanwise direction and 1.27 cm (.5 in.) in the radial direction.

Figures 46 and 50 show velocity and pressure contours for a Dean number of 50. Patterns are roughly spanwise uniform with some scatter which probably results from noise intermixed with the extremely low levels of pressure measured.

Figures 47, 48, 49, 51, 52 and 53 are velocity and pressure contours for Dean numbers 75, 100 and 150, respectively. Both velocity and pressure contours show nearly spanwise uniform characteristics with deficits appearing occasionally near the concave surface. The deficits correspond to time-averaged position, of vortex upwash regions where relatively low-velocity/low-pressure fluid is swept away from the concave walls by secondary flows.

IV. SUMMARY AND CONCLUSIONS

Studies are conducted using two curved channels with identical internal dimensions. One channel is used for flow visualization, and one channel is used for heat transfer measurements. Both channels have mild curvature, 40 to 1 aspect ratio, and a 1.27 cm by 50.80 cm (.5 in. by 20 in.) interior cross section.

Portions of the final assembly of the heat transfer channel are completed. This assembly includes installation of insulation to minimize conductive heat transfer to the environment and completion of wiring of 204 thermocouples used for measurement of surface temperature, mixed mean inlet temperature, mixed mean outlet temperature and ambient temperatures in the vicinity of the test section. Also complete is the wiring of heating power supplies, including controlling systems, as well as installation of regulating valves and flow metering orifices.

Velocity and pressure surveys are presented from measurements in the heat transfer channel 19 cm downstream from the heated section. For Dean numbers 50 to 158, these distributions are nearly spanwise uniform, as expected, providing qualification of the internal flow behavior in the heat transfer channel.

Flow visualization results are presented as obtained in the transparent curved channel for Dean numbers 60 to 200 and angular positions from 85 ° to 185 ° from the start of curvature. At the channel inlet, smoke is introduced into the lower half. In the curved section, the smoke then travels principally along the convex wall until rearranged and redistributed by centrifugal instabilities. Dean vortices are observed for angular positions of 85 ° to 155 ° and Dean numbers greater than 75. The unsteadiness of these vortices increases with Dean number and angular position. Vortex pairs are observed to engulf adjacent vortices as Dean number and angular position increase. This occurs as the 'petal' of one vortex pair wraps around the neighboring vortex pair allowing their common upwash regions to merge. Other types of unsteady Dean vortex pair behavior are also observed including spanwise oscillations, radial oscillations, twisting, vortex pair expansion and vortex pair contraction.

TC #	X (cm)	Z (cm)	TC #	X (cm)	Z (cm)
1	15.24	15.36	26	106.68	.119
2	15.24	.119	27	106.68	-15.36
3	15.24	-15.12	28	137.16	15.36
4	45.72	15.36	29	137.16	.119
5	45.72	.119	30	137.16	-15.12
6	45.72	-15.12	31	167.64	15.36
7	76.20	15.36	32	167.64	1.897
8	76.20	.119	33	167.64	1.643
9	76.20	-15.12	34	167.64	1.389
10	106.68	15.36	35	167.64	1.135
11	106.68	.119	36	167.64	.881
12	106.68	-15.12	37	167.64	.627
13	137.16	15.36	38	167.64	.373
14	137.16	.119	39	167.64	.119
15	137.16	-15.12	40	167.64	-.135
16	15.24	15.36	41	167.64	-.389
17	15.24	.119	42	167.64	-.643
18	15.24	-15.12	43	167.64	-.897
19	45.72	15.36	44	167.64	-1.151
20	45.72	.119	45	167.64	-1.405
21	45.72	-15.12	46	167.64	-1.659
22	76.20	15.36	47	167.64	-15.12
23	76.20	.119	48	198.12	15.36
24	76.20	-15.12	49	198.12	1.897
25	106.68	15.36	50	198.12	1.643

Table 1. THERMOCOUPLE LOCATIONS

TC #	X (cm)	Z (cm)	TC #	X (cm)	Z (cm)
51	198.12	1.389	76	228.60	-.643
52	198.12	1.135	77	228.60	-.897
53	198.12	.881	78	228.60	-1.151
54	198.12	.627	79	228.60	-1.405
55	198.12	.373	80	228.60	-1.659
56	198.12	.119	81	228.60	-15.12
57	198.12	-.135	82	259.08	15.36
58	198.12	-.389	83	259.08	1.897
59	198.12	-.643	84	259.08	1.643
60	198.12	-.897	85	259.08	1.389
61	198.12	-1.151	86	259.08	1.135
62	198.12	-1.405	87	259.08	.881
63	198.12	-1.659	88	259.08	.627
64	198.12	-15.12	89	259.08	.373
65	228.60	15.36	90	259.08	.119
66	228.60	1.897	91	259.08	-.135
67	228.60	1.643	92	259.08	-.389
68	228.60	1.389	93	259.08	-.643
69	228.60	1.135	94	259.08	-.897
70	228.60	.881	95	259.08	-1.151
71	228.60	.627	96	259.08	-1.405
72	228.60	.373	97	259.08	-1.659
73	228.60	.119	98	259.08	-15.12
74	228.60	-.135	99	289.56	15.36
75	228.60	-.389	100	289.56	1.897

Table 2. THERMOCOUPLE LOCATIONS (CONTINUED)

TC #	X (cm)	Z (cm)	TC #	X (cm)	Z (cm)
101	289.56	1.897	126	167.64	-.389
102	289.56	1.389	127	167.64	-.643
103	289.56	1.1352	128	167.64	-.897
104	289.56	.881	129	167.64	-1.151
105	289.56	.627	130	167.64	-1.405
106	289.56	.373	131	167.64	-1.659
107	289.56	.119	132	167.64	-15.12
108	289.56	-.135	133	198.12	15.36
109	289.56	-.3892	134	198.12	1.897
110	289.56	-.643	135	198.12	1.643
111	289.56	-.897	136	198.12	1.389
112	289.56	-1.151	137	198.12	1.135
113	289.56	-1.405	138	198.12	.881
114	289.56	-1.659	139	198.12	.627
115	289.56	-15.12	140	198.12	.373
116	167.64	15.36	141	198.12	.119
117	167.64	1.897	142	198.12	-.135
118	167.64	1.643	143	198.12	-.389
119	167.64	1.389	144	198.12	-.643
120	167.64	1.135	145	198.12	-.897
121	167.64	.881	146	198.12	-1.151
122	167.64	.627	147	198.12	-1.405
123	167.64	.373	148	198.12	-1.659
124	167.64	.119	149	198.12	-15.12
125	167.64	-.135	150	228.60	15.36

Table 3. THERMOCOUPLE LOCATIONS (CONTINUED)

TC #	X (cm)	Z (cm)	TC #	X (cm)	Z (cm)
151	228.60	1.897	176	259.08	-.135
152	228.60	1.643	177	259.08	-.3896
153	228.60	1.389	178	256.08	-.643
154	228.60	1.135	179	259.08	-.897
155	228.60	.881	180	259.08	-1.151
156	228.60	.627	181	259.08	-1.405
157	228.60	.3736	182	259.08	-1.659
158	228.60	.119	183	259.08	-15.12
159	228.60	-.135	184	289.56	15.36
160	228.60	-.389	185	289.56	1.897
161	228.60	-.643	186	289.56	1.643
162	228.60	-.897	187	289.56	1.389
163	228.60	-1.151	188	289.56	1.135
164	228.60	-1.405	189	289.56	.881
165	228.60	-1.659	190	289.56	.627
166	228.60	-15.12	191	289.56	.373
167	256.08	15.36	192	289.56	.119
168	259.08	1.897	193	289.56	-.135
169	259.08	1.643	194	289.56	-.389
170	259.08	1.389	195	289.56	-.6435
171	259.08	1.135	196	289.56	-.897
172	259.08	.881	197	289.56	-1.151
173	259.08	.627	198	289.56	-1.405
174	259.08	.373	199	289.56	-1.659
175	259.08	.119	200	289.56	-15.12

Table 4. THERMOCOUPLE LOCATIONS (CONTINUED)

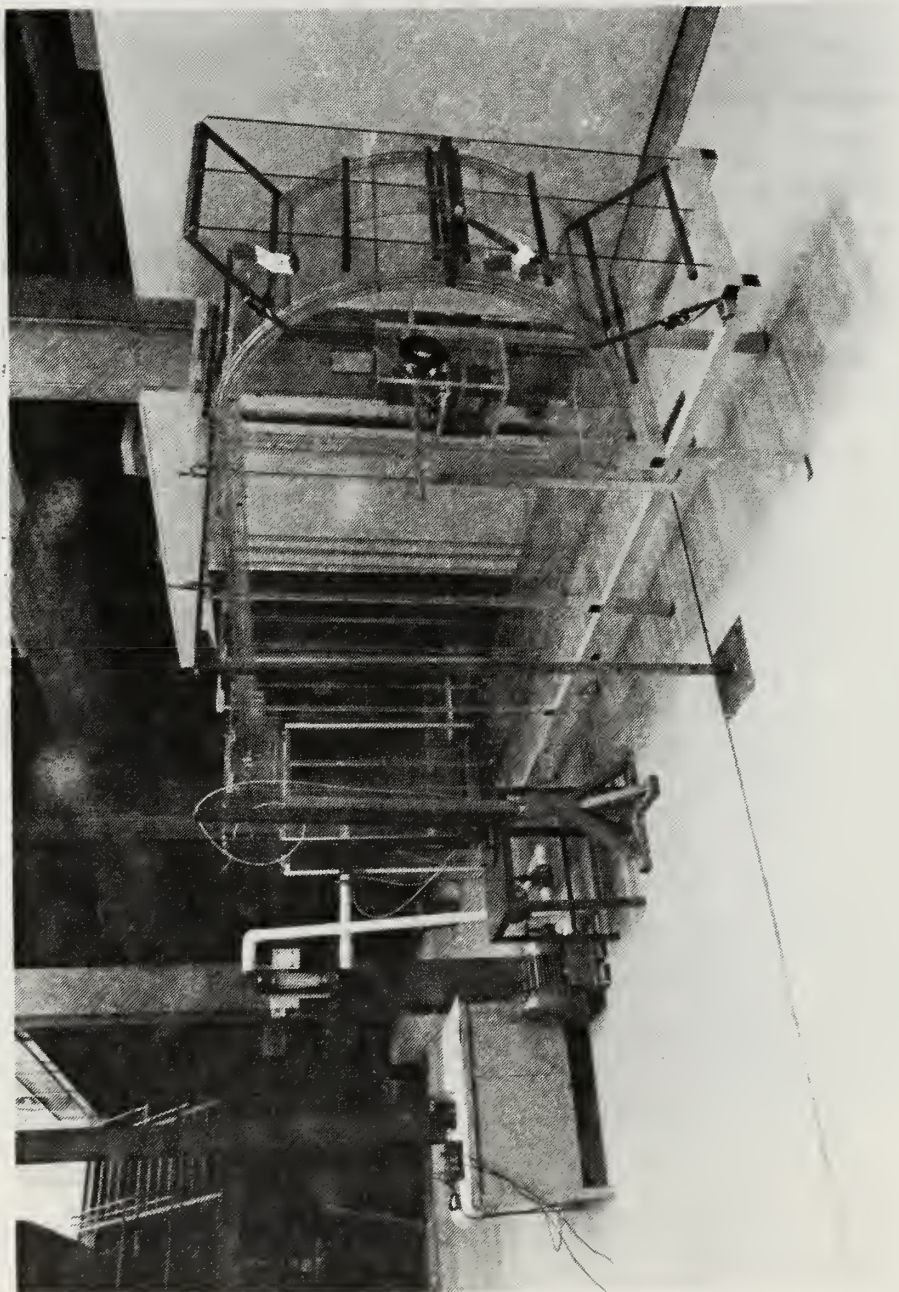


Figure 1. Transparent Channel

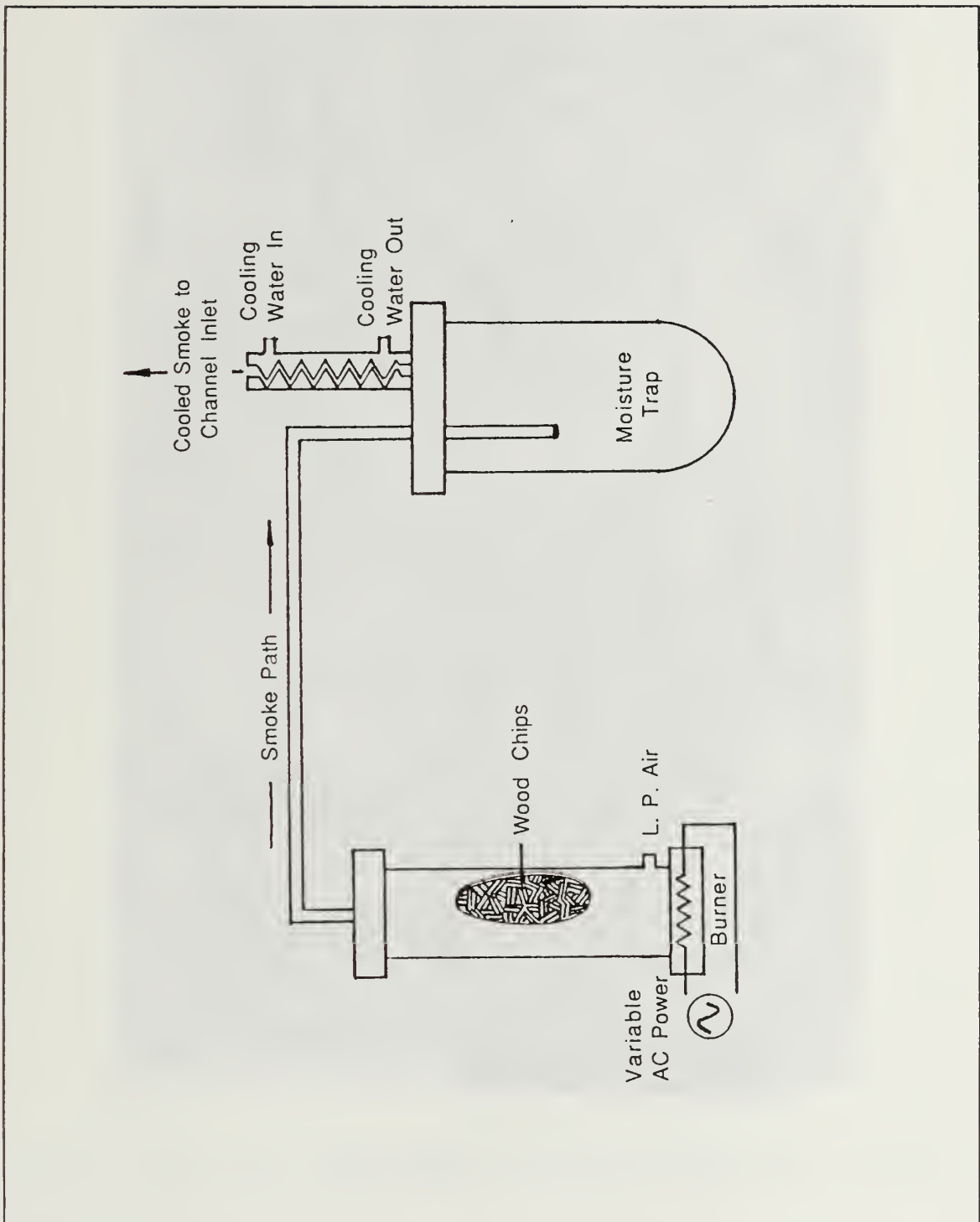


Figure 2. Smoke Generator

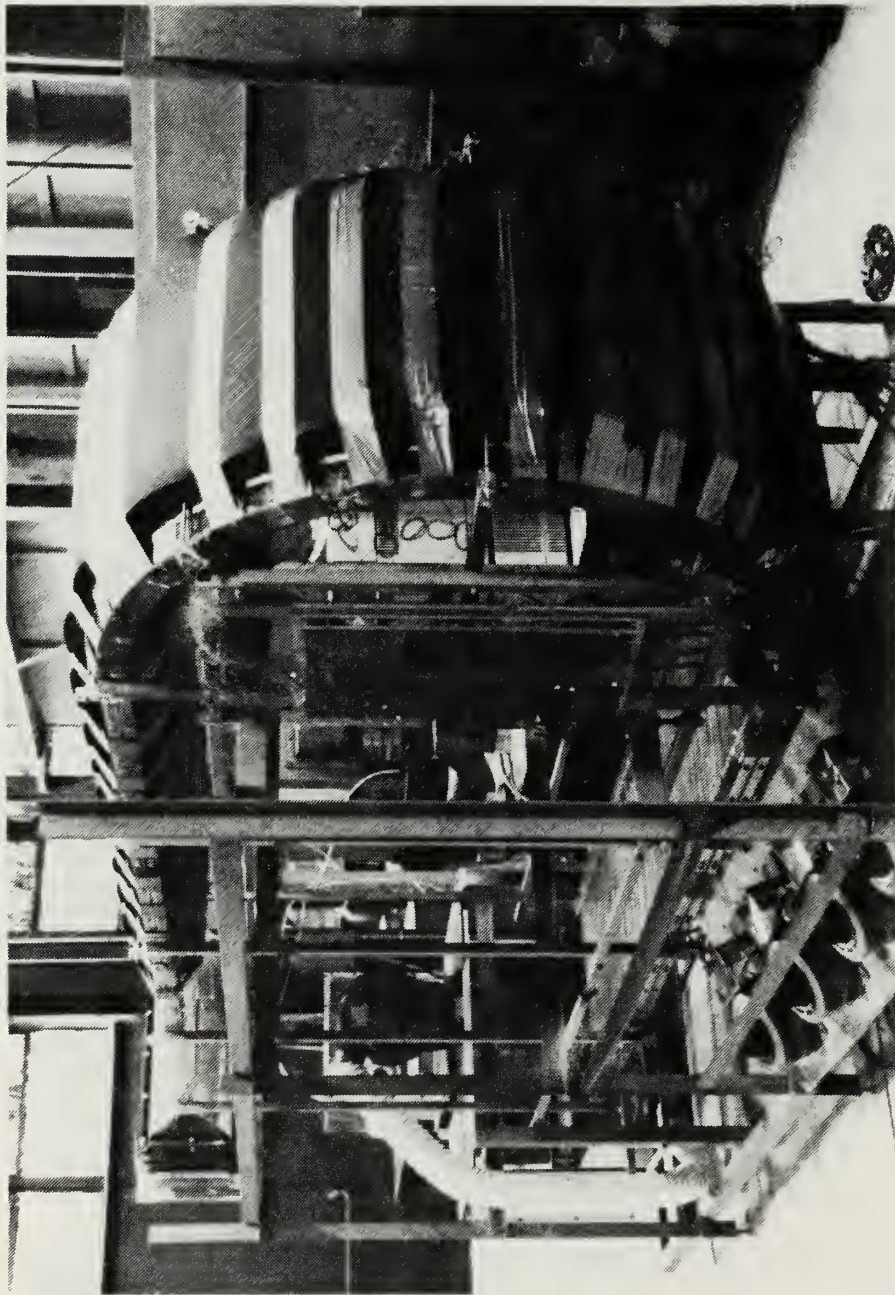


Figure 3. Heat Transfer Channel Rear Quarter View

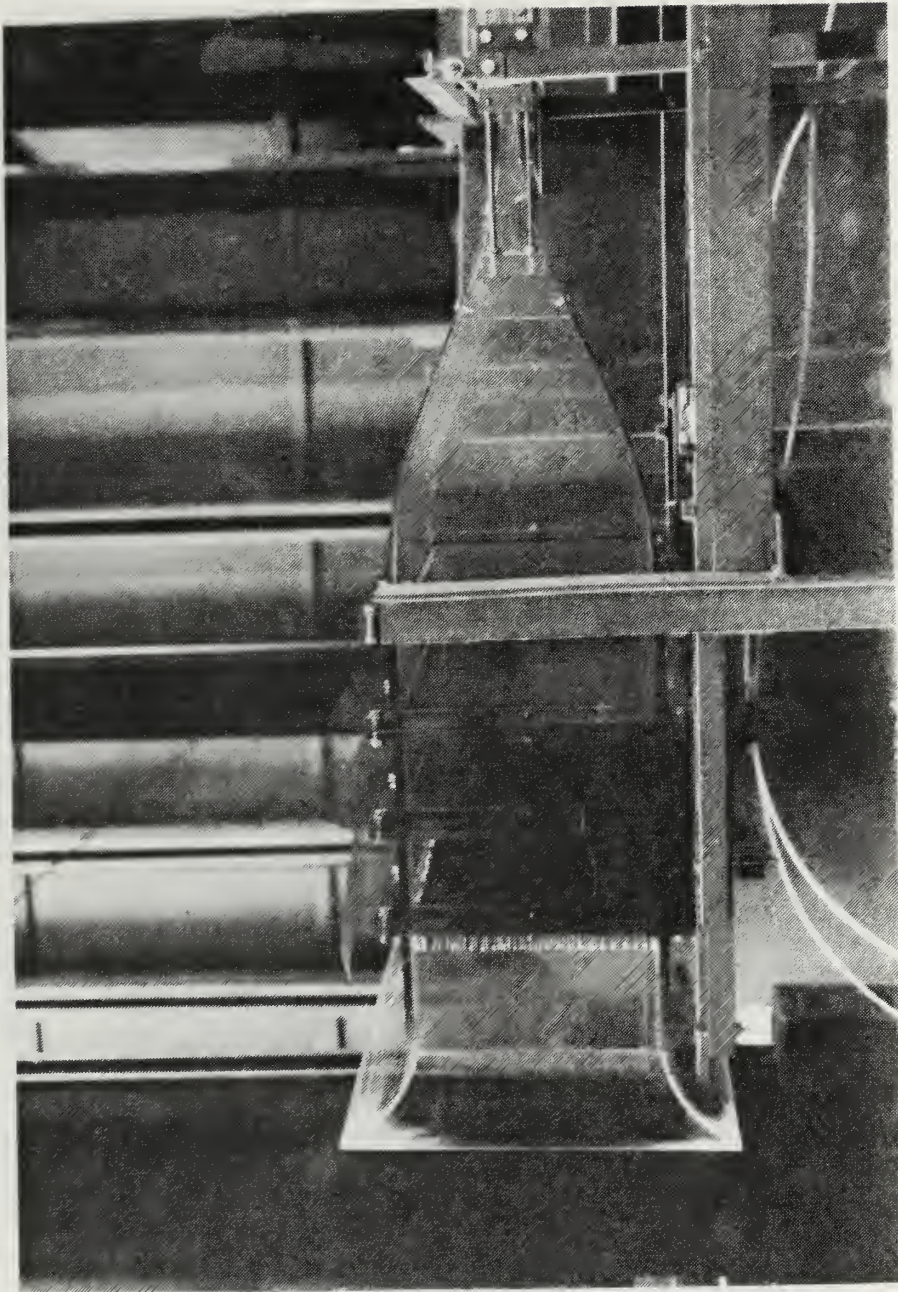


Figure 4. Heat Transfer Channel Inlet

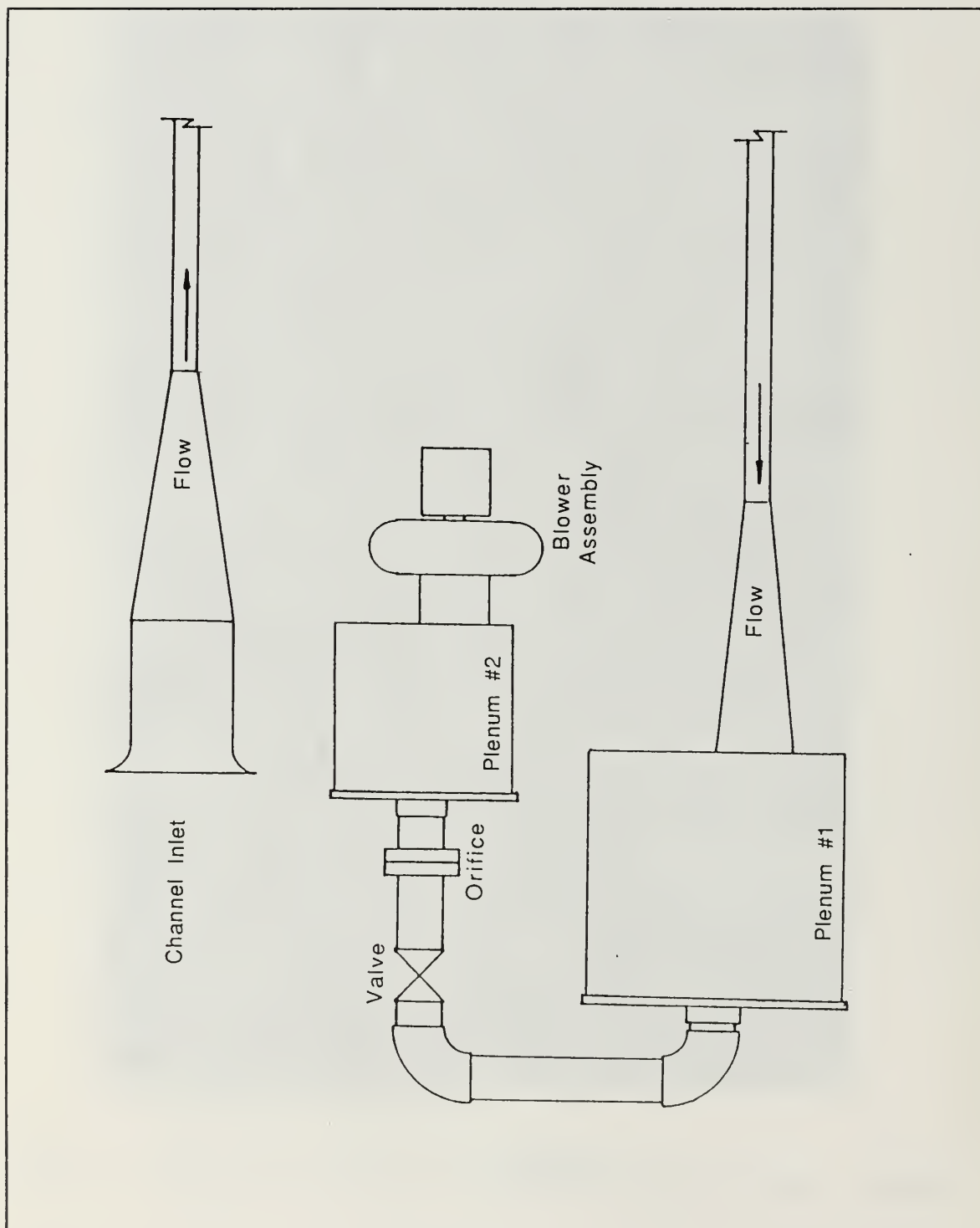


Figure 5. Arrangement drawing of blower, plenum #1 and #2, orifice and globe valve.

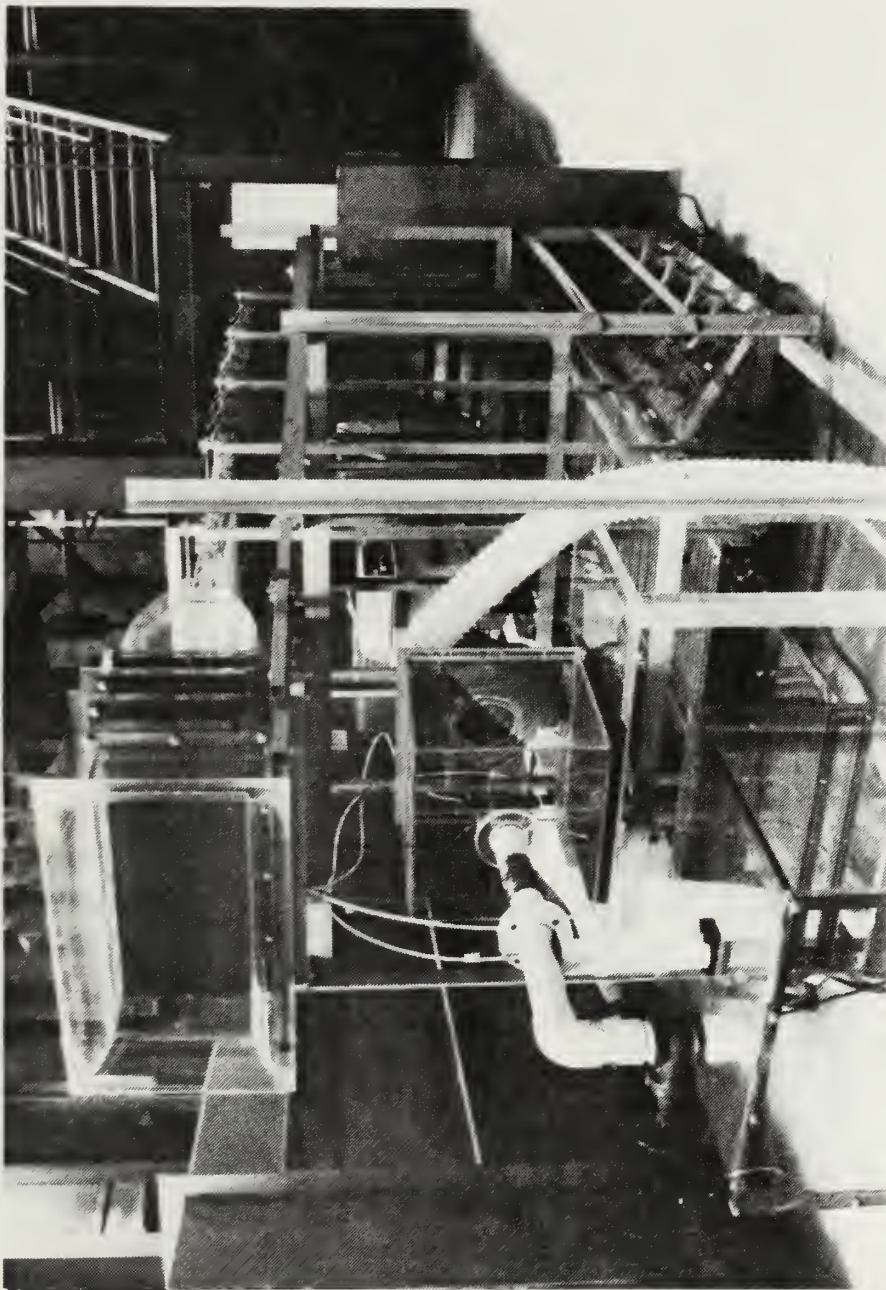


Figure 6. Heat Transfer Channel Front Quarter View

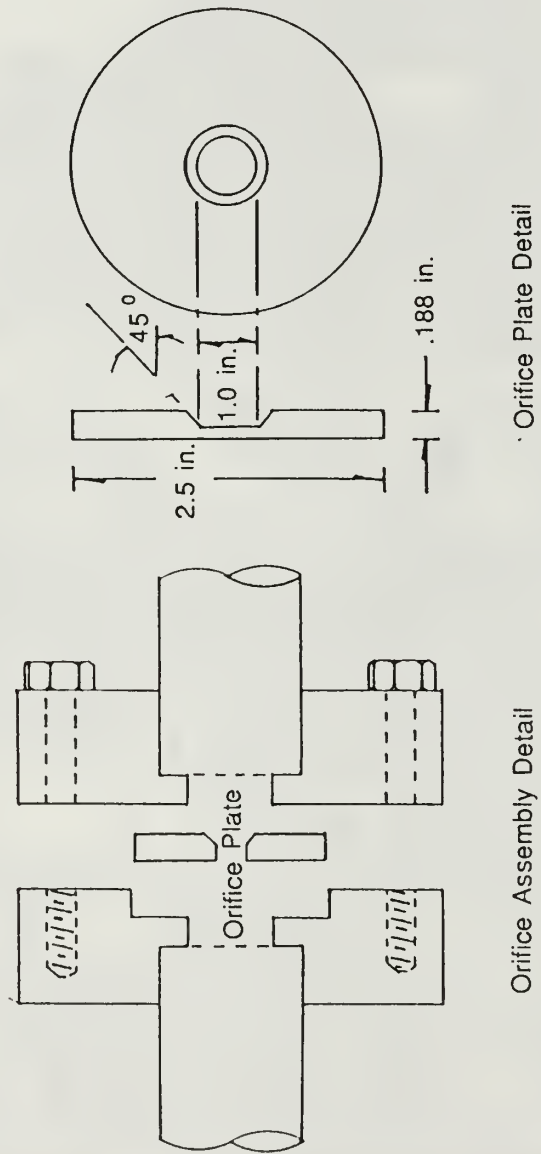


Figure 7. Orifice Plate Assembly Details

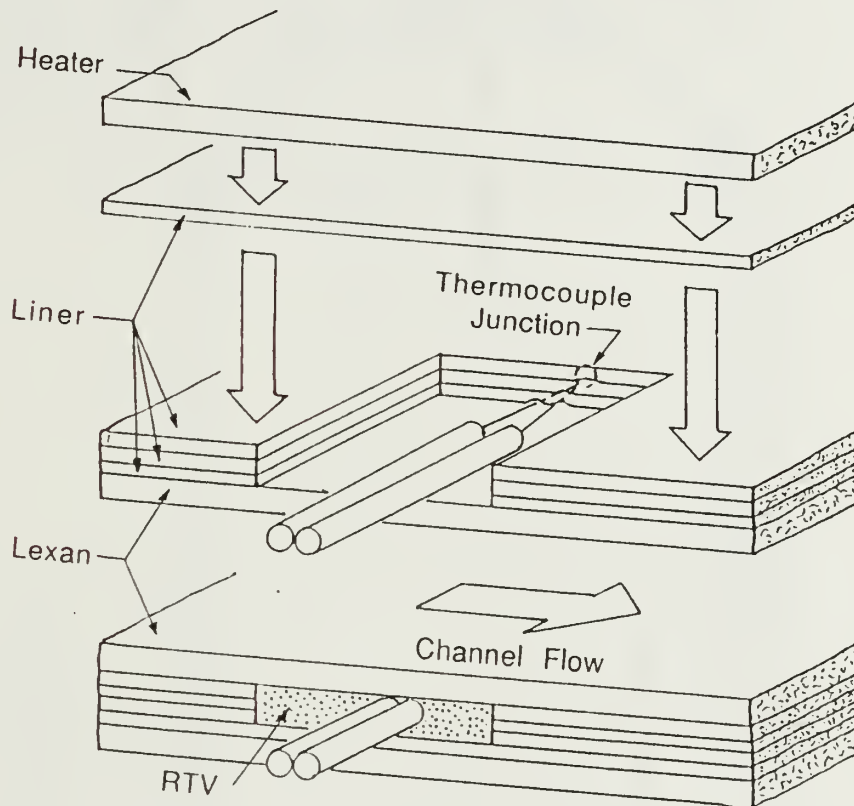


Figure 8. Heat Transfer Channel Thermocouple Installation

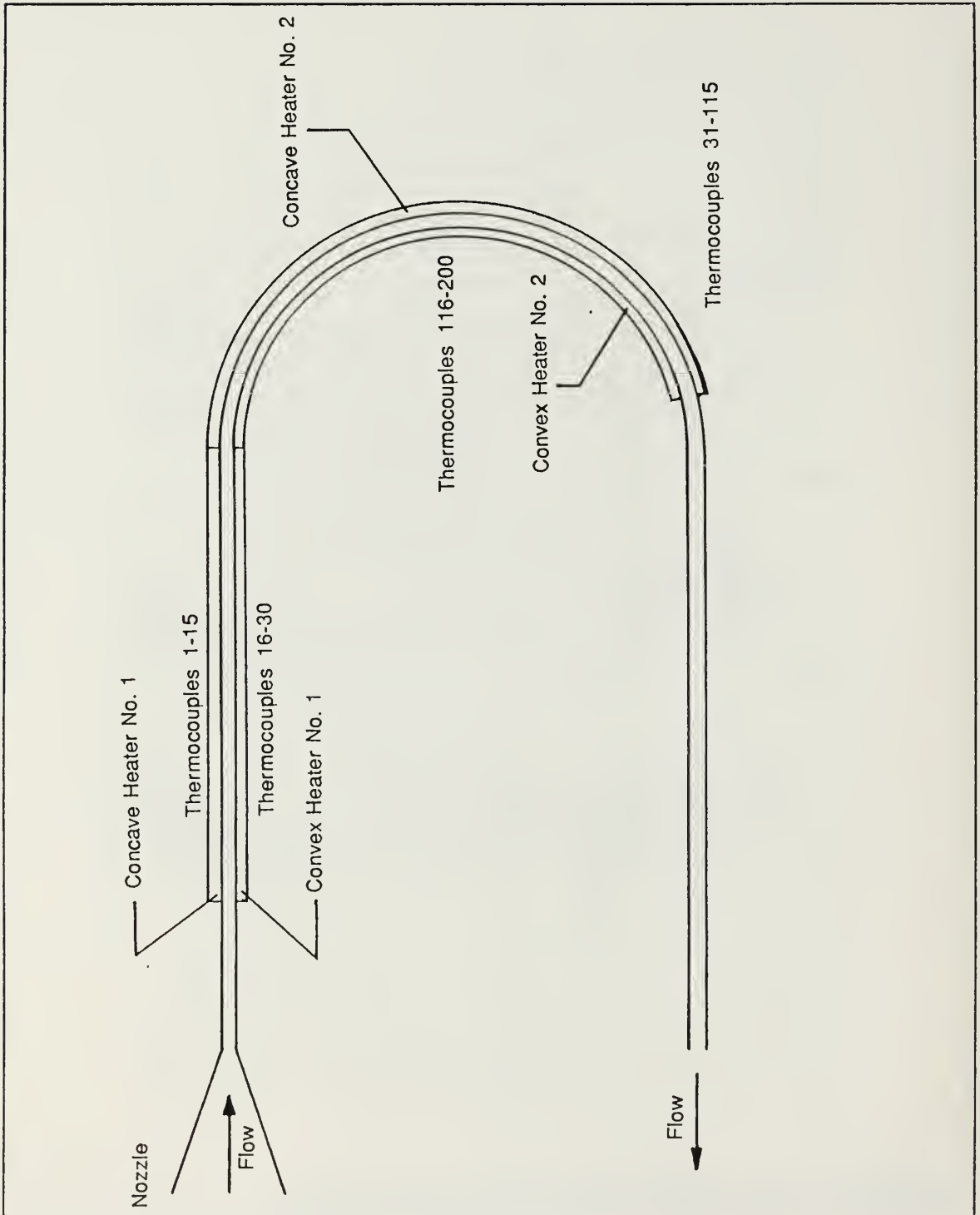


Figure 9. Heat Transfer channel Heater Identification

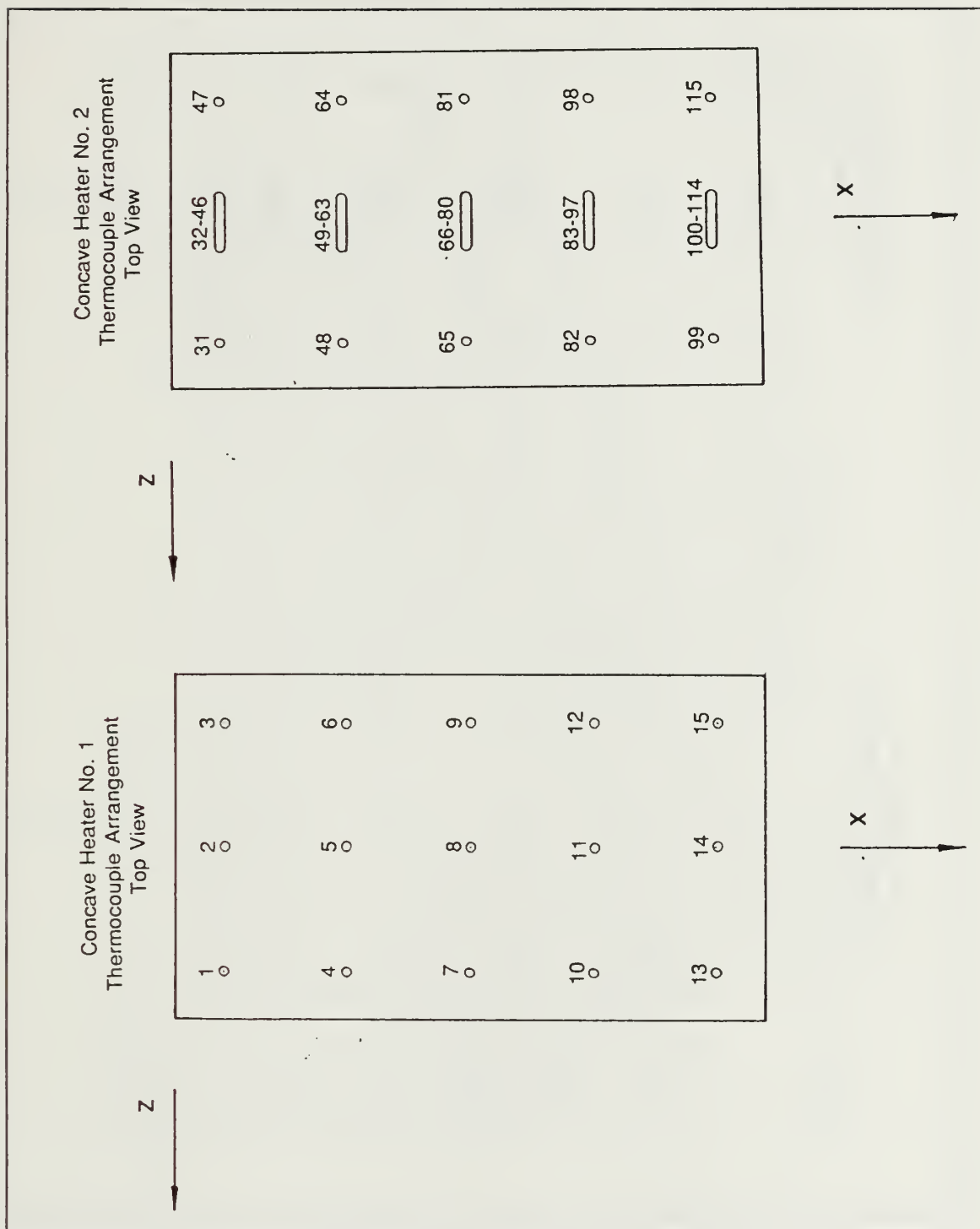


Figure 10. Concave Heater Thermocouple Placement

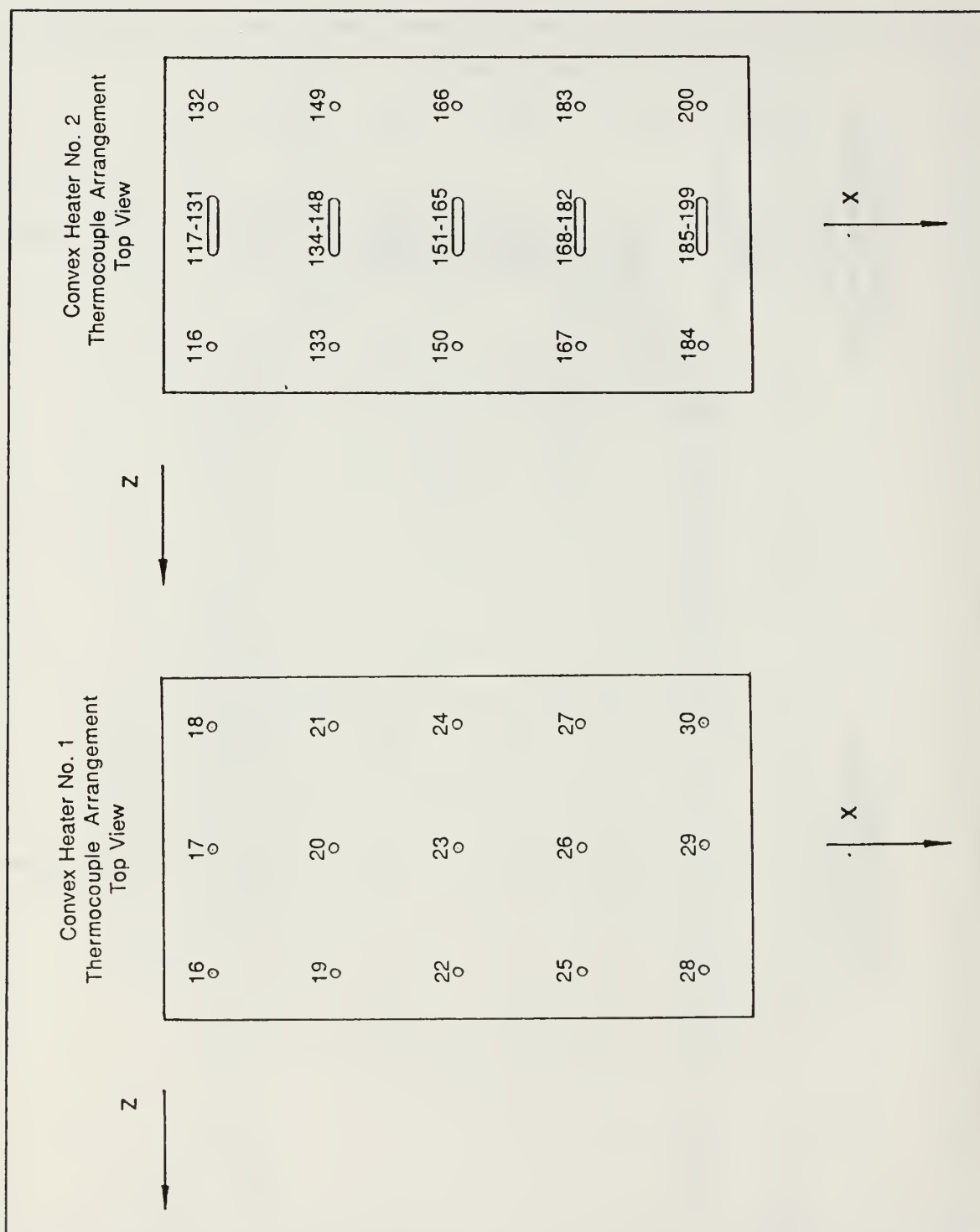


Figure 11. Convex Heater Thermocouple Placement

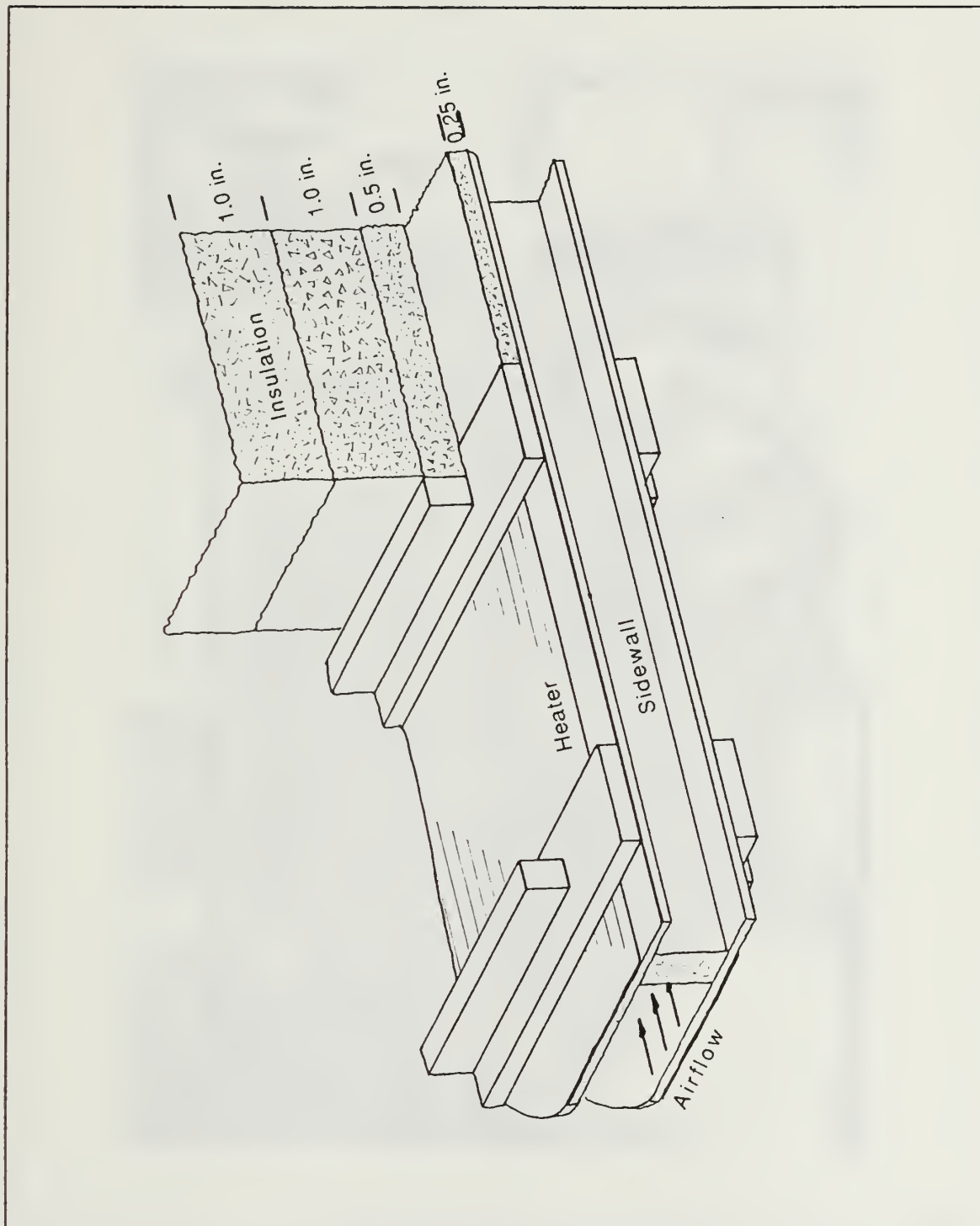


Figure 12. Heat Transfer Channel Insulation Drawing

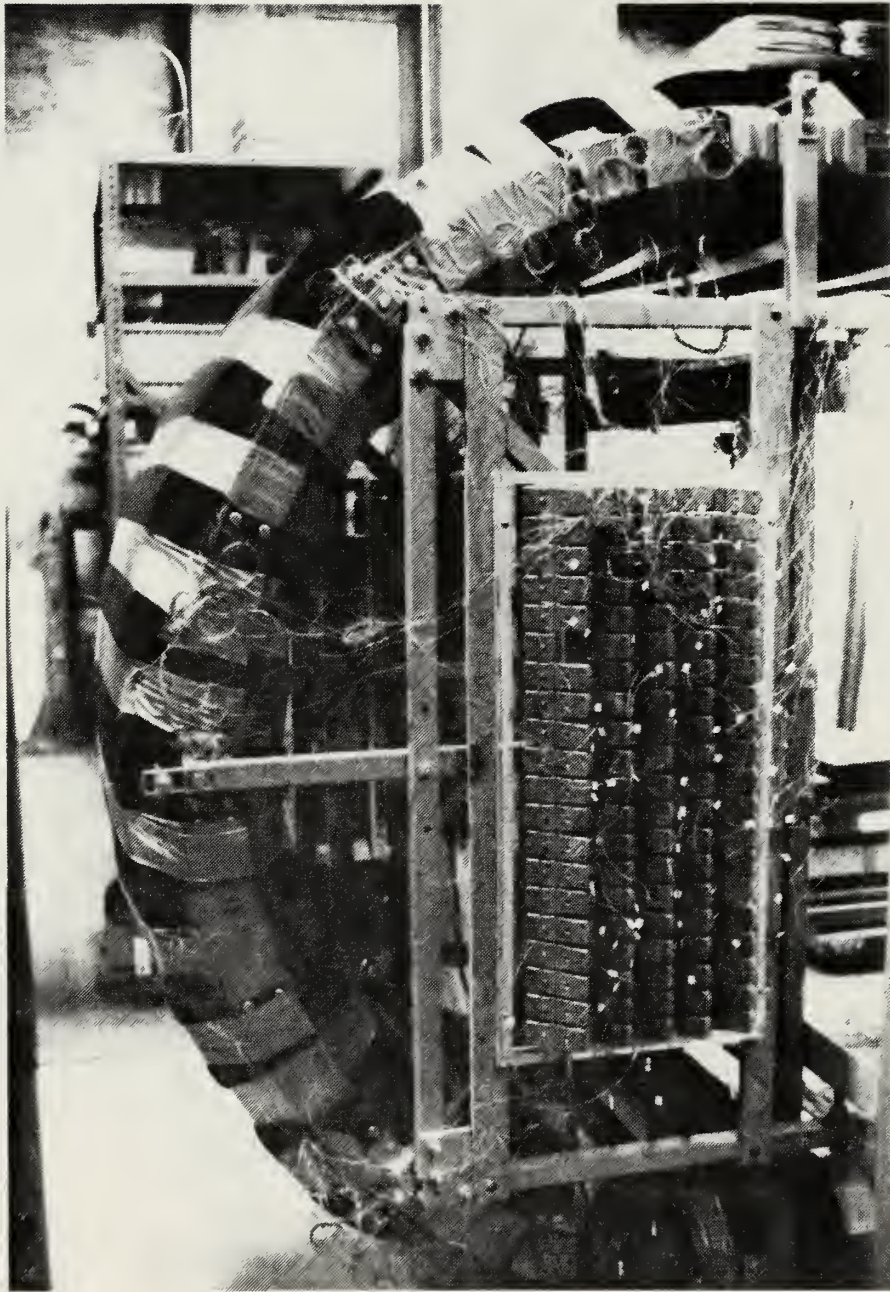


Figure 13. Heat Transfer Channel Insulation Photograph

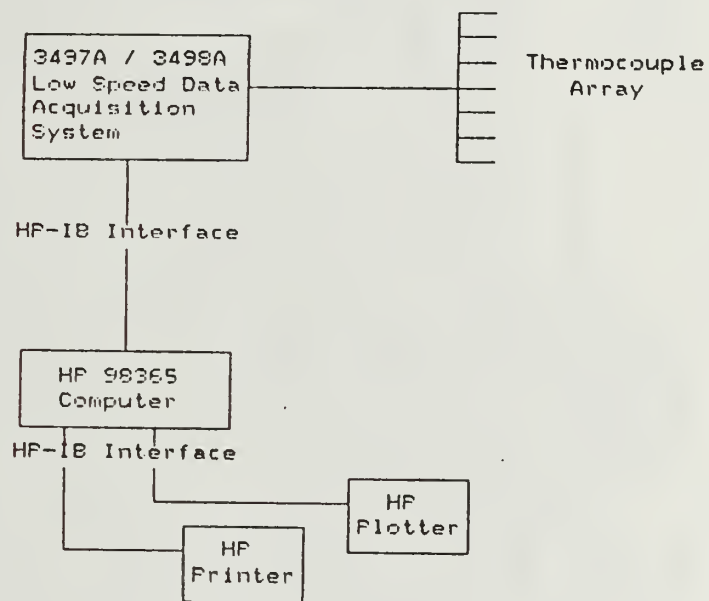


Figure 14. Heat Transfer Channel Data Acquisition System for Temperature Measurement

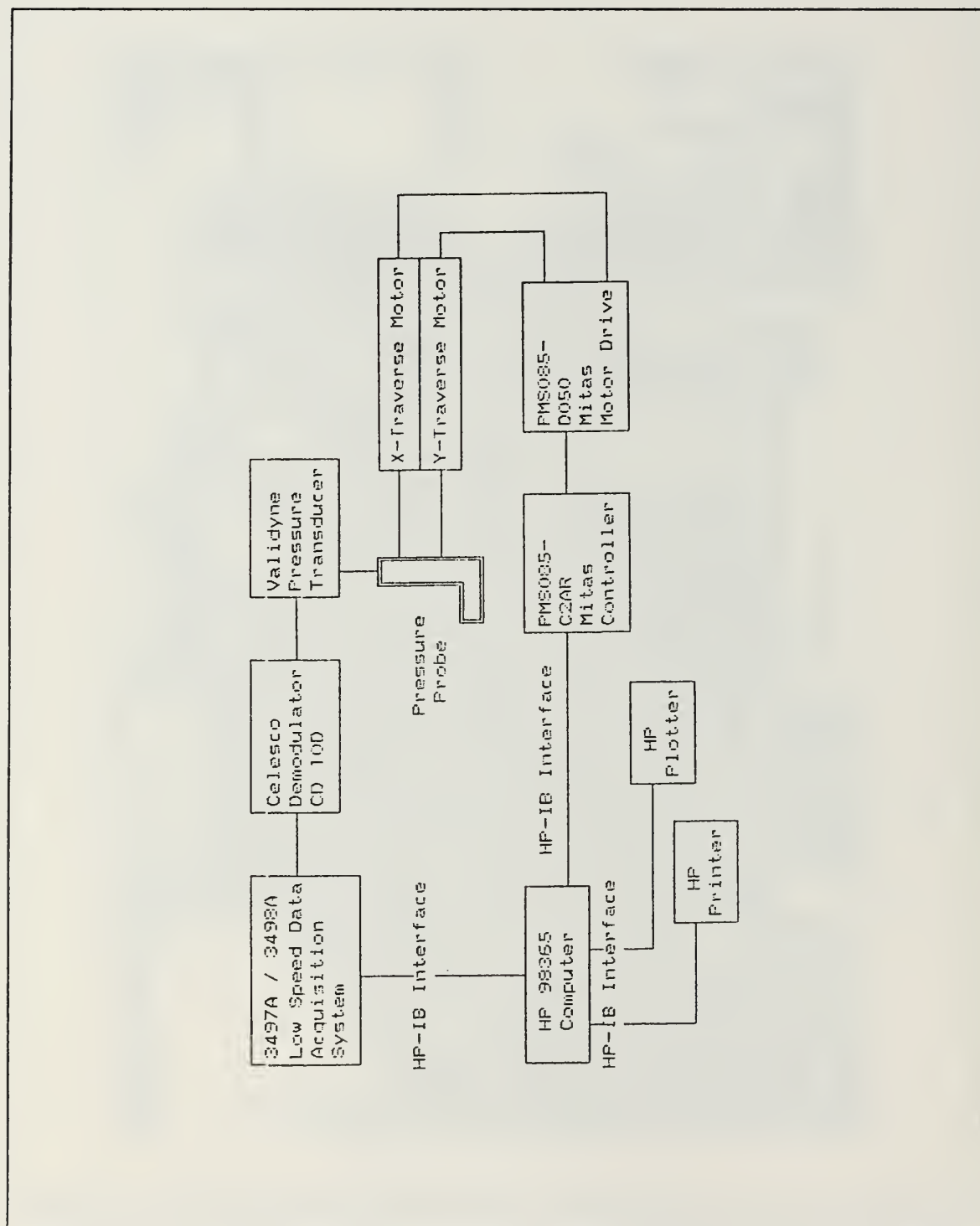


Figure 15. Heat Transfer Channel Data Acquisition System for Flow Measurement

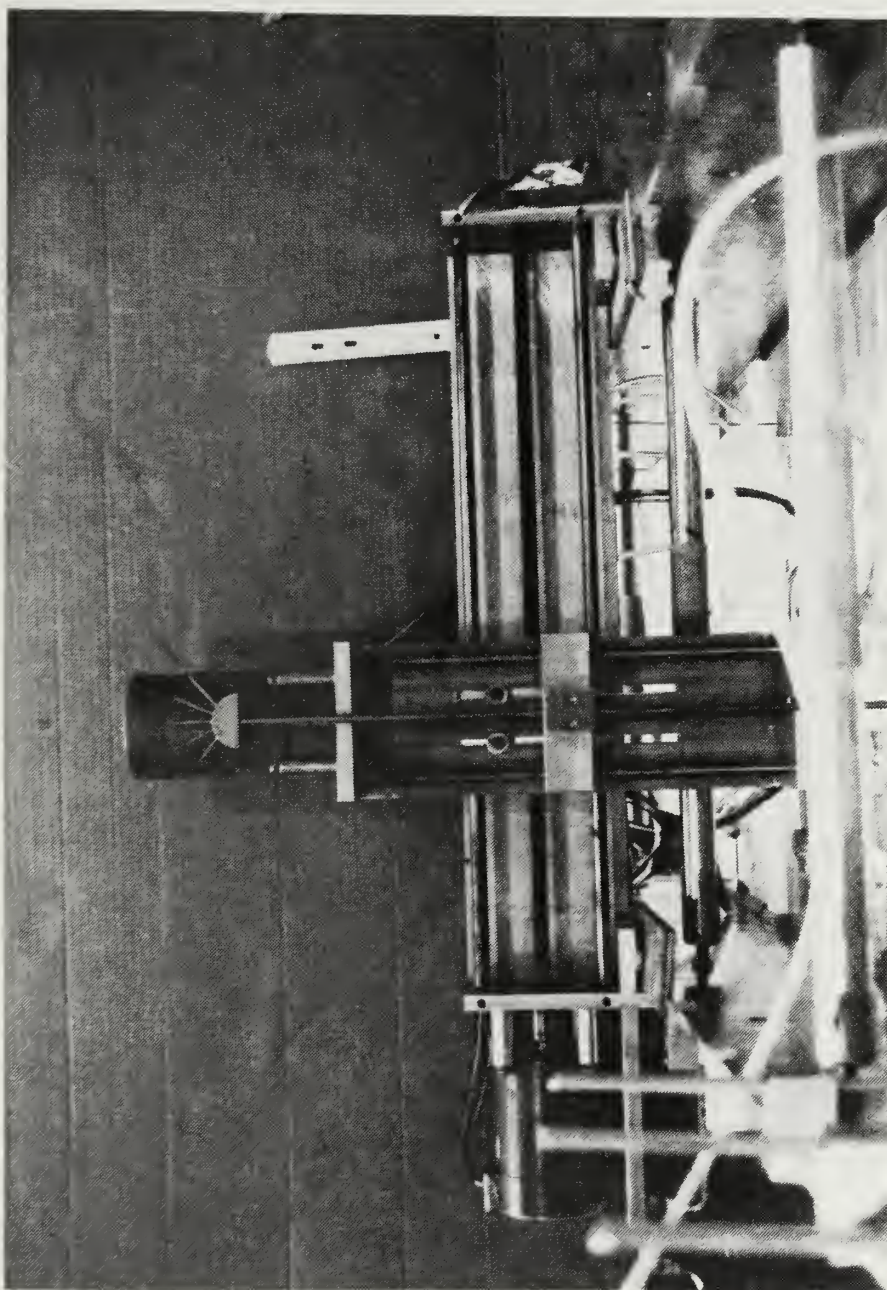


Figure 16. Traversing Mechanism

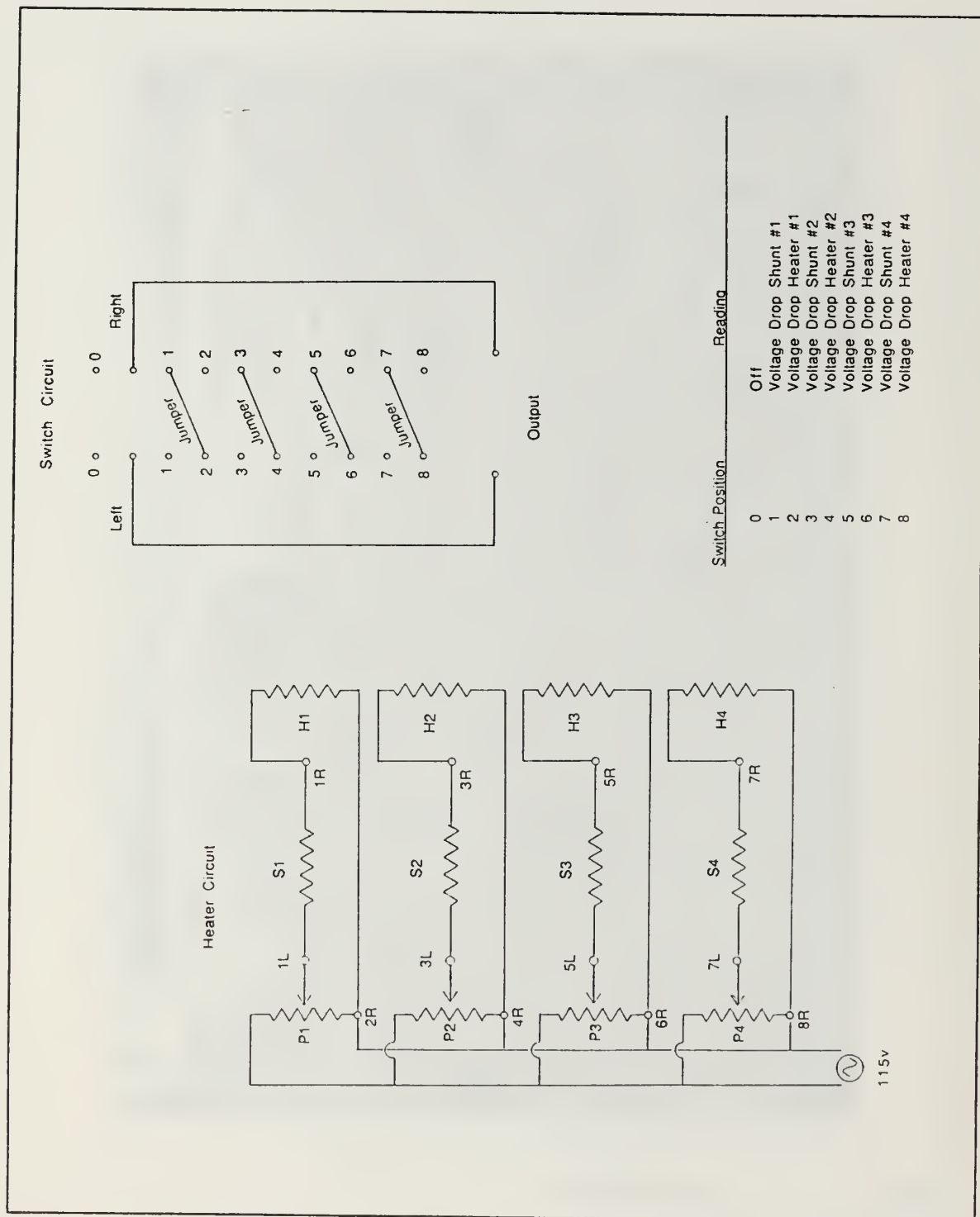


Figure 17. Heater and Control Circuit Wiring Diagram

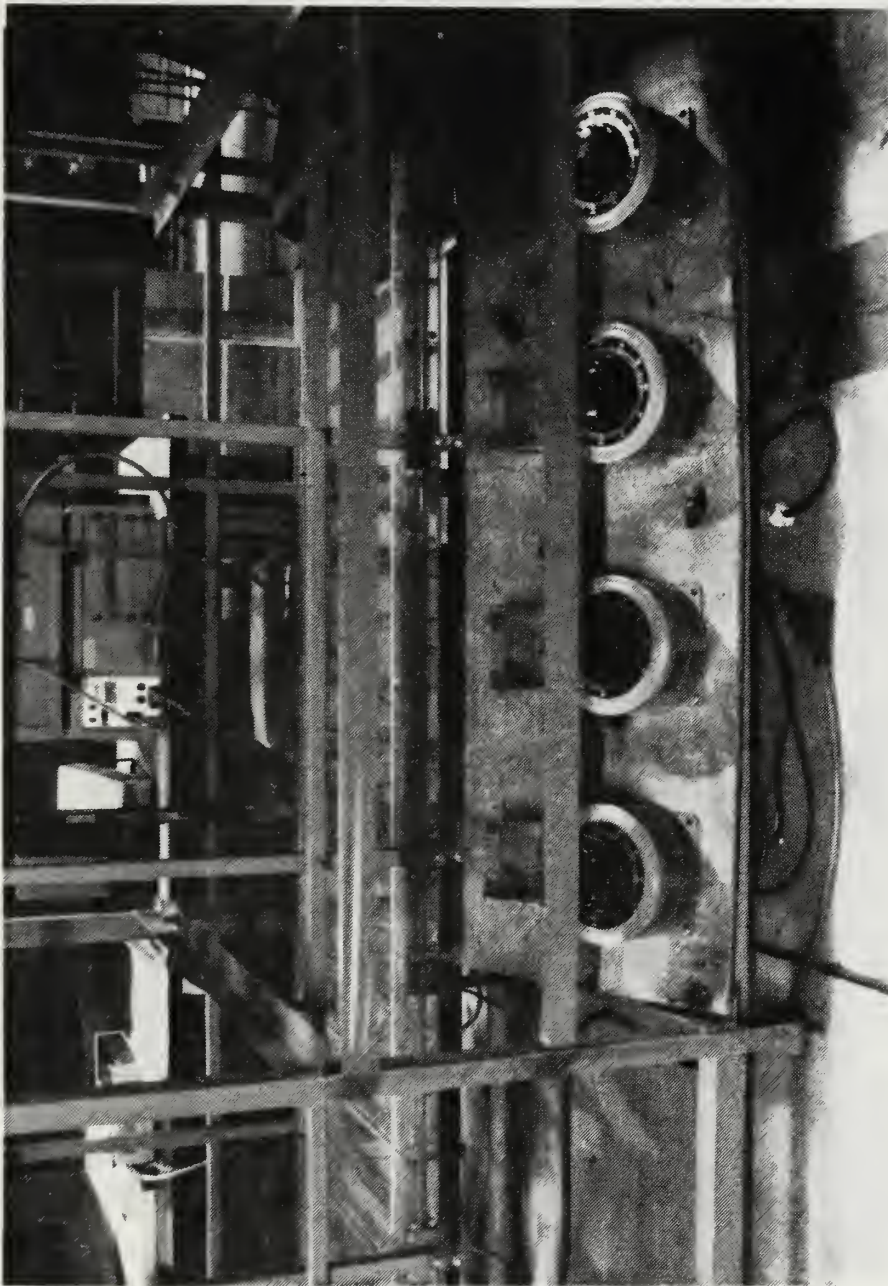


Figure 18. Heat Transfer Channel Heater Control Variacs

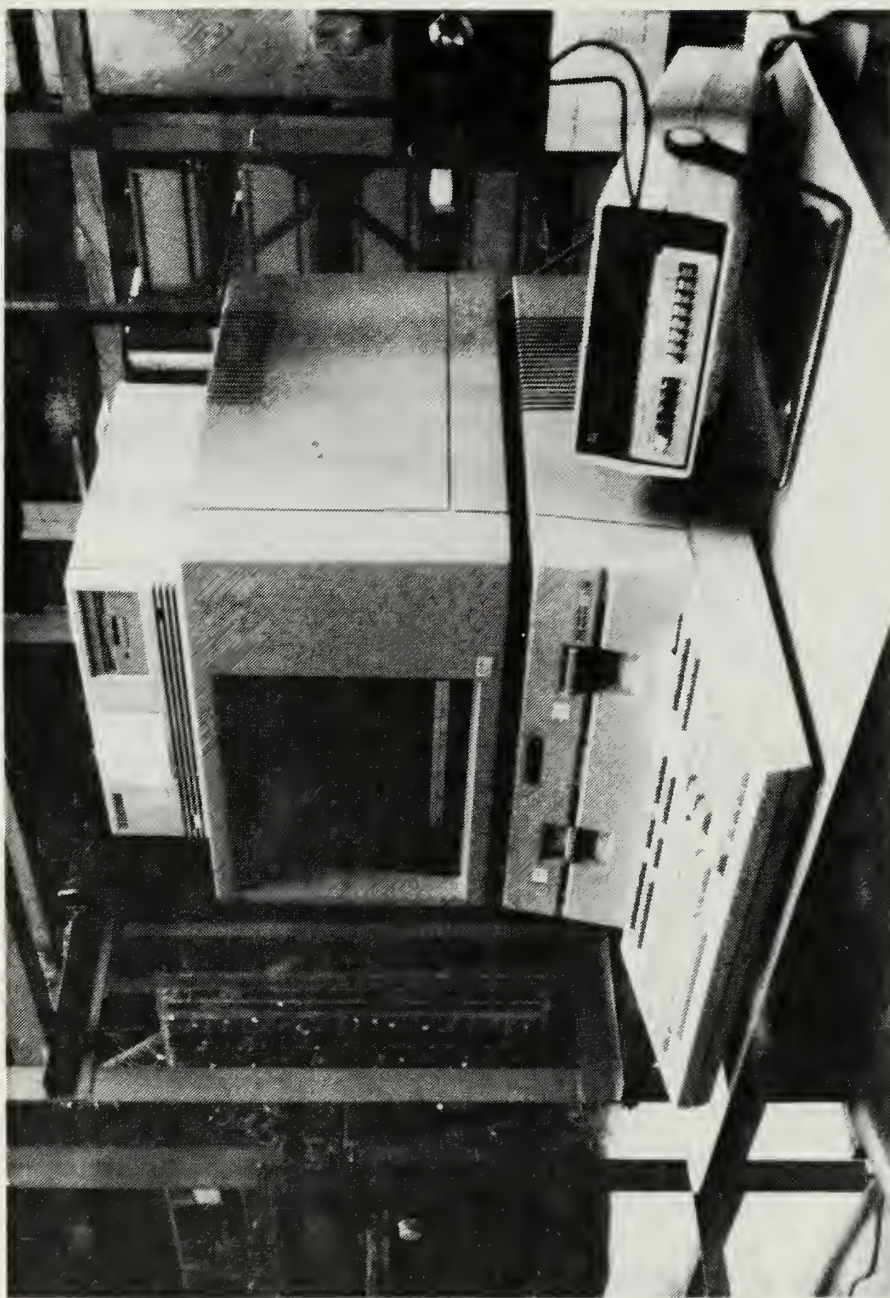


Figure 19. Operator Station

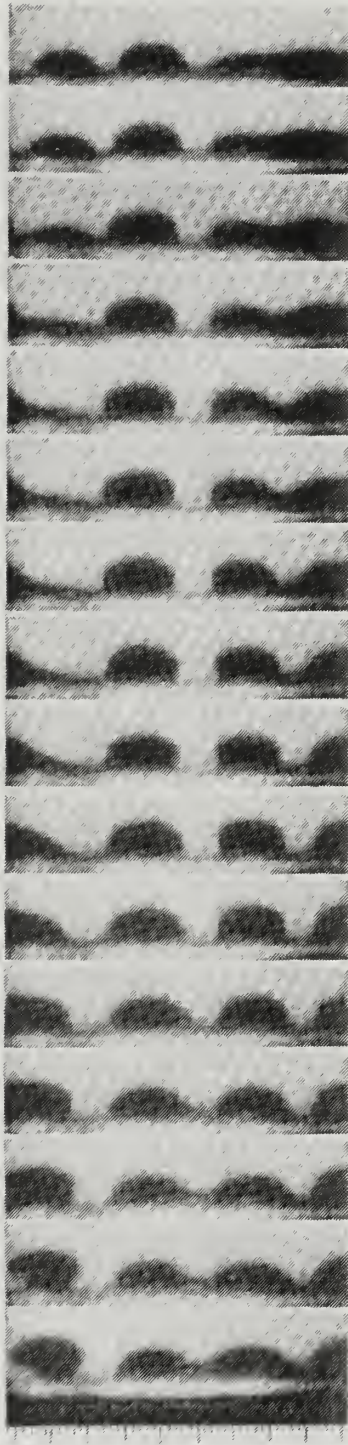


Figure 20. Flow Visualization Results $De = 75$ $\theta = 85^\circ$

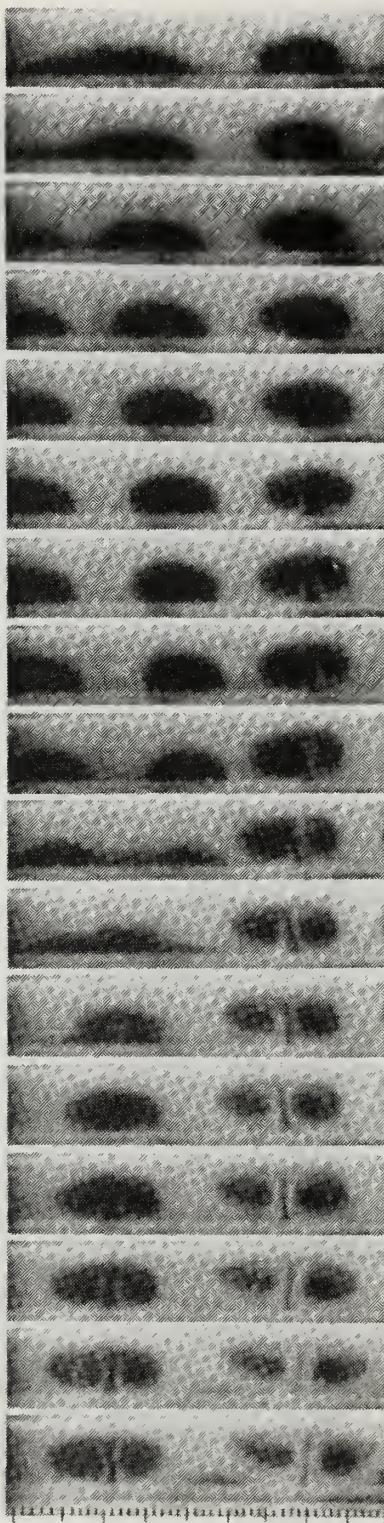


Figure 21. Flow Visualization Results $De = 75$ $\theta = 95^\circ$

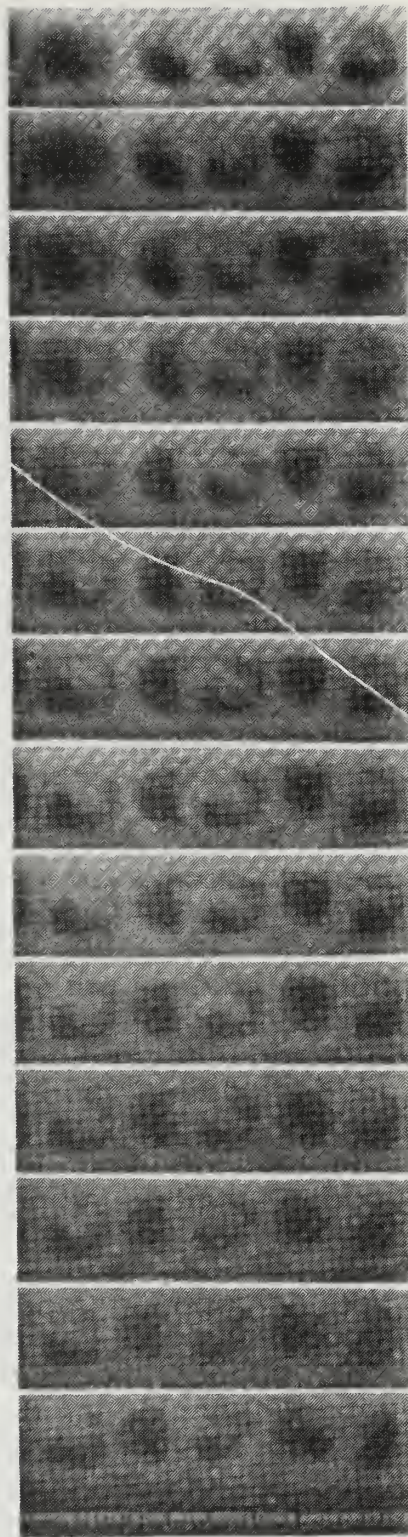


Figure 22. Flow Visualization Results $De = 75$ $\theta = 135^\circ$ (1 of 10)

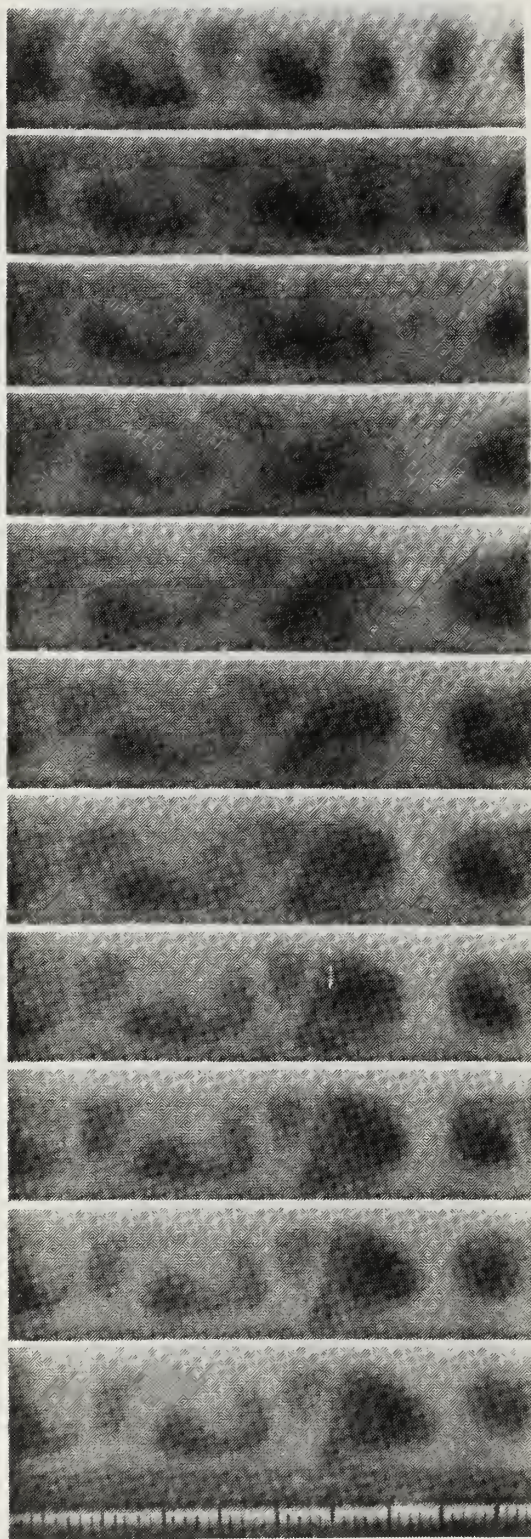


Figure 23. Flow Visualization Results $De = 75$ $\theta = 135^\circ$ (2 of 10)

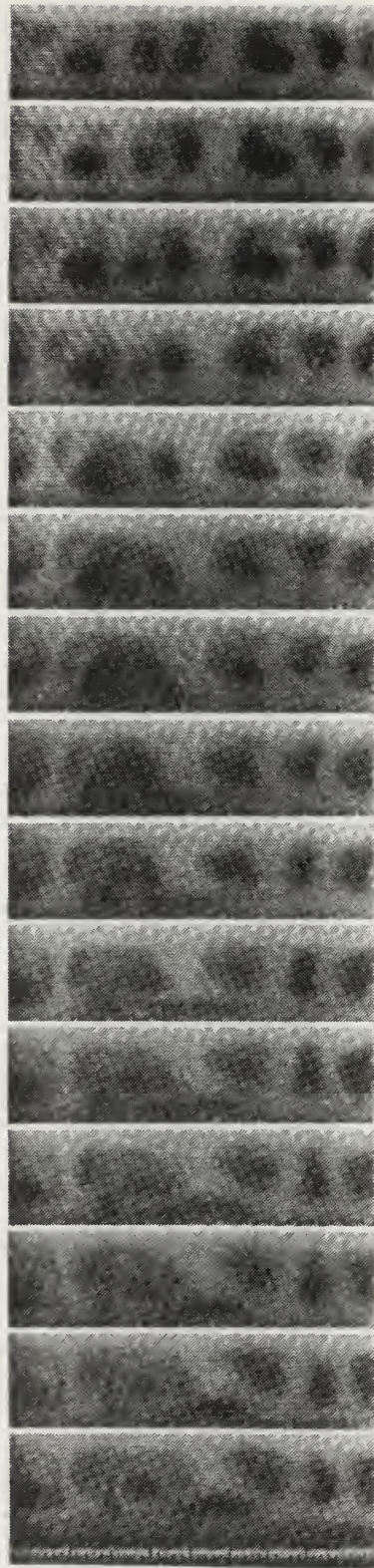


Figure 24. Flow Visualization Results $De = 75$ $\theta = 135^\circ$ (3 of 10)

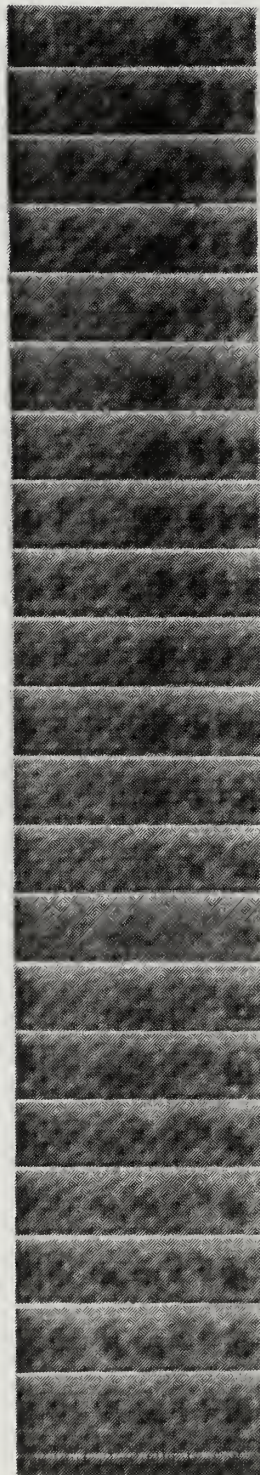


Figure 25. Flow Visualization Results $De = 75$ $\theta = 135^\circ$ (4 of 10)

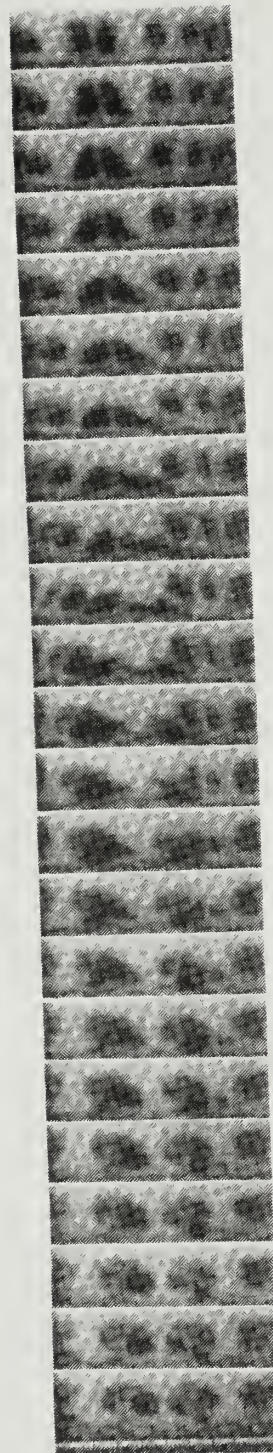


Figure 26. Flow Visualization Results $De = 75$ $\theta = 135^\circ$ (5 of 10)

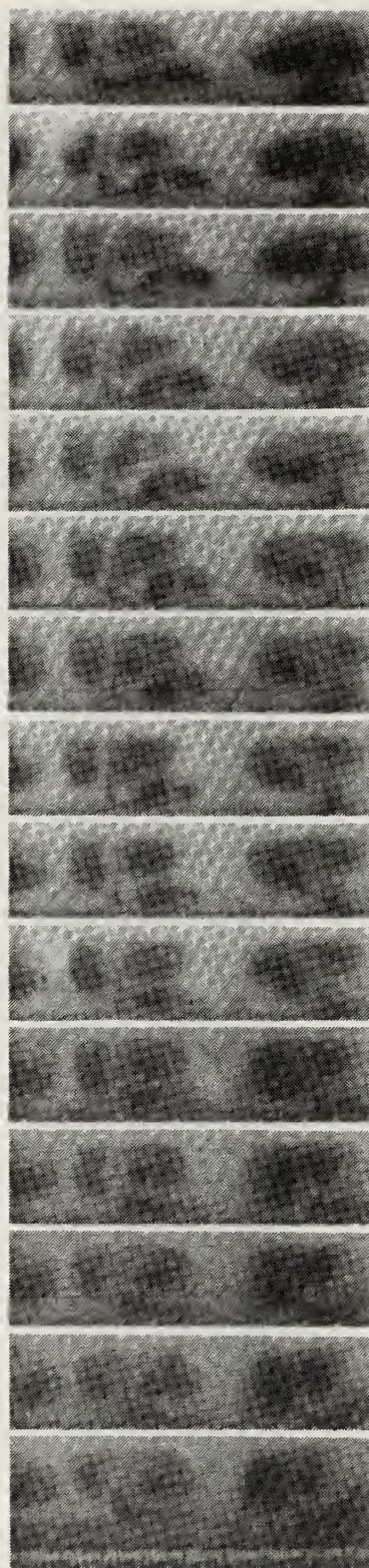


Figure 27. Flow Visualization Results $De = 75$ $\theta = 135^\circ$ (6 of 10)

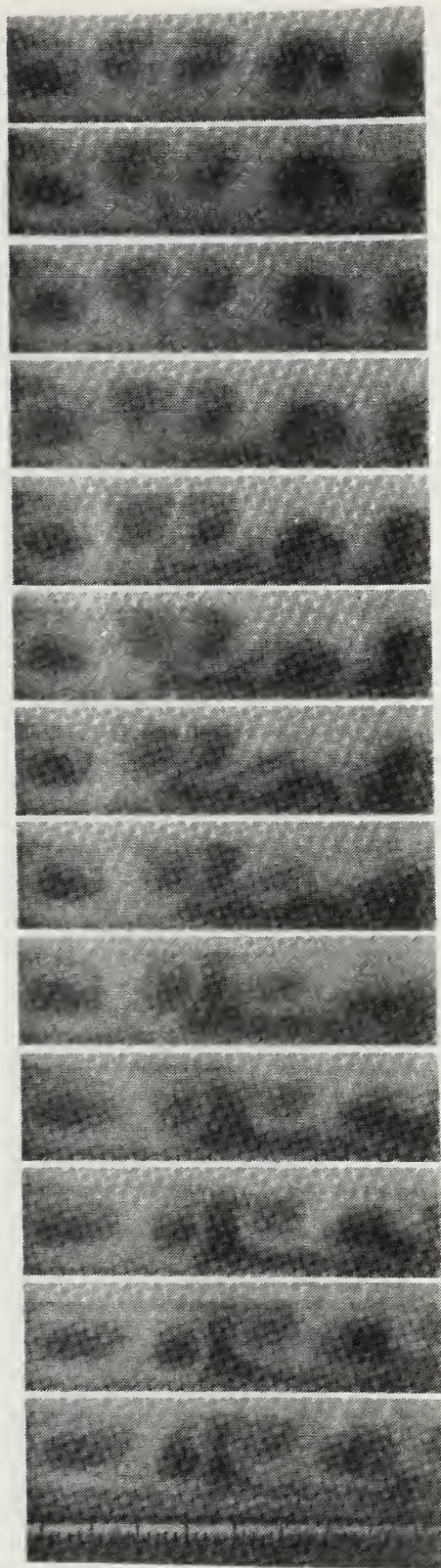


Figure 28. Flow Visualization Results $De = 75$ $\theta = 135^\circ$ (7 of 10)

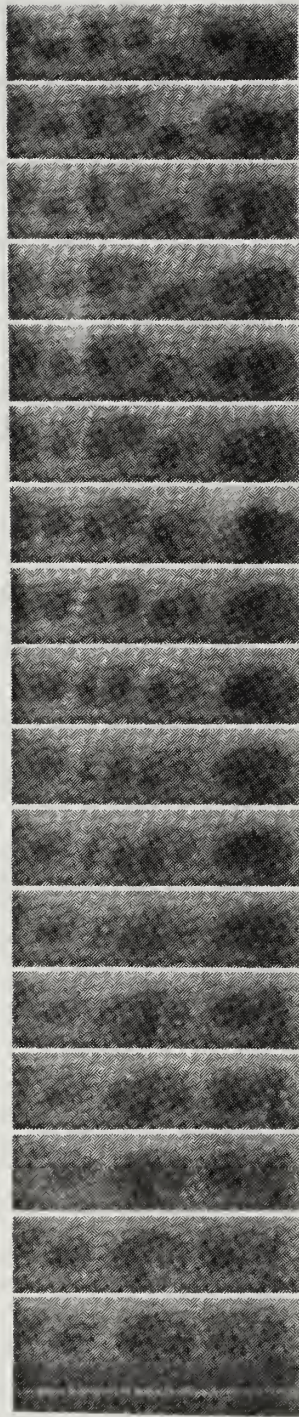


Figure 29. Flow Visualization Results $De = 75$ $\theta = 135^\circ$ (8 of 10)

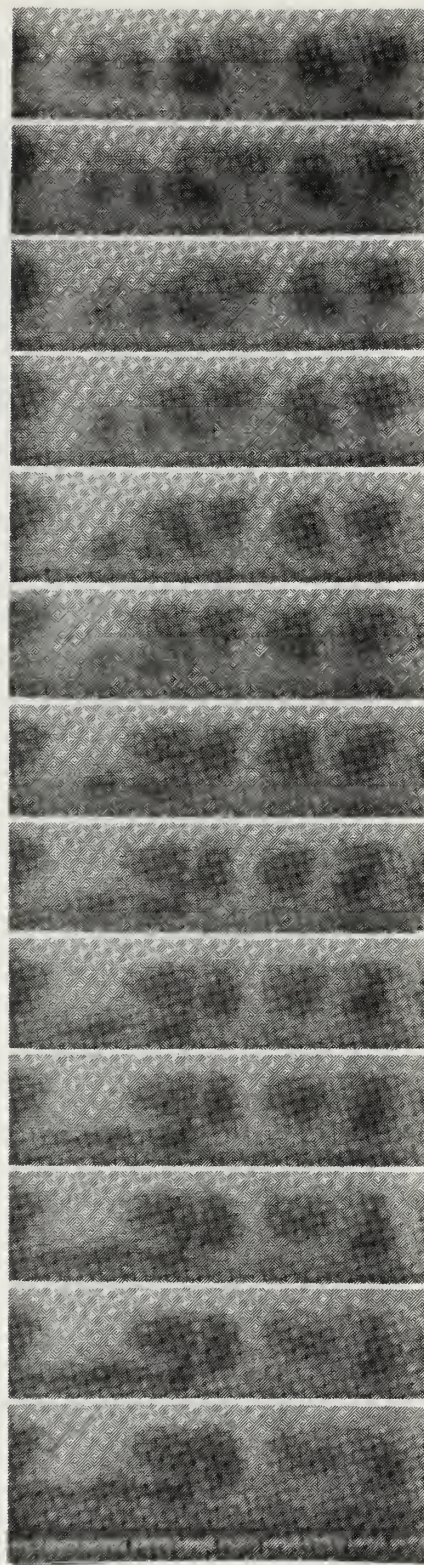


Figure 30. Flow Visualization Results $De = 75$ $\theta = 135^\circ$ (9 of 10)

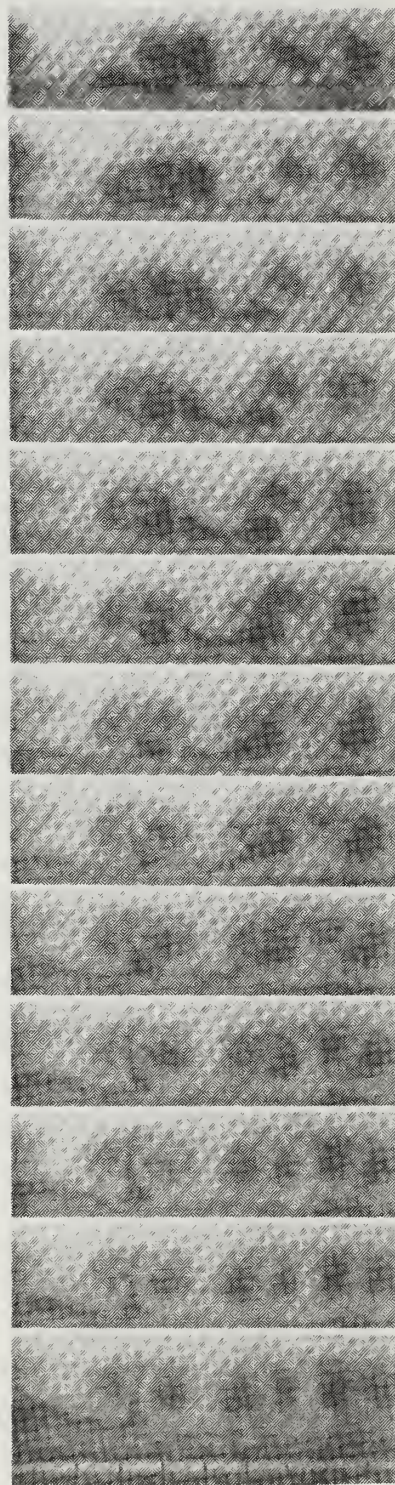


Figure 31. Flow Visualization Results $De = 75$ $\theta = 135^\circ$ (10 of 10)

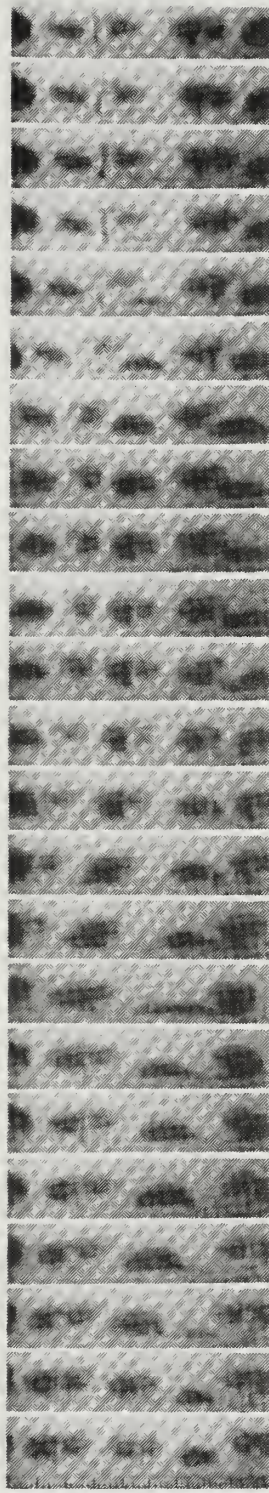


Figure 32. Flow Visualization Results $De = 100$ $\theta = 95^\circ$

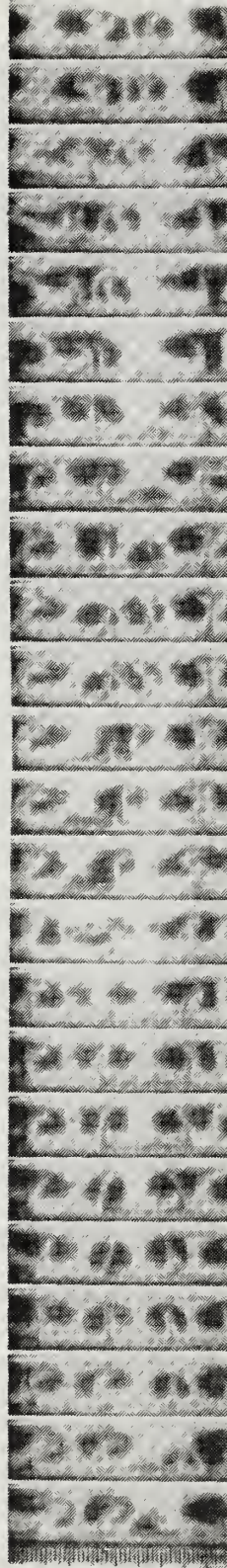


Figure 33. Flow Visualization Results $De = 100$ $\theta = 105^\circ$

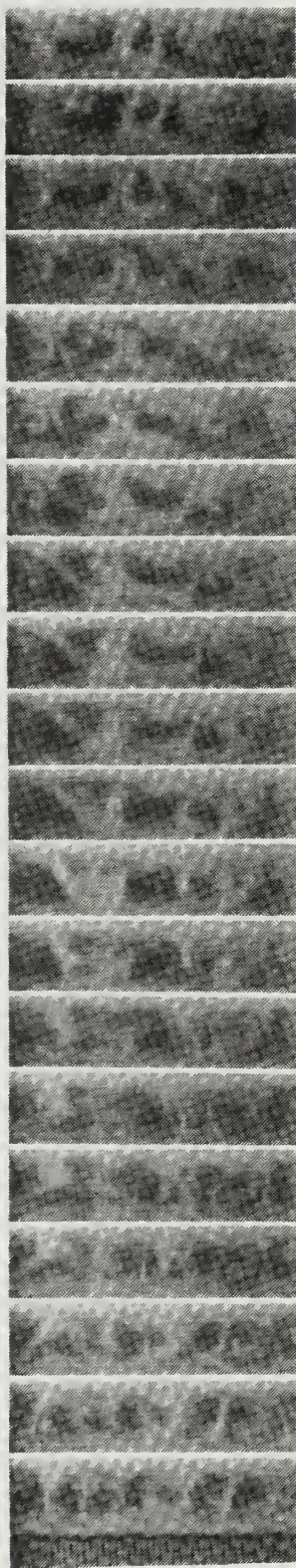


Figure 34. Flow Visualization Results $De = 100$ $\theta = 145^\circ$

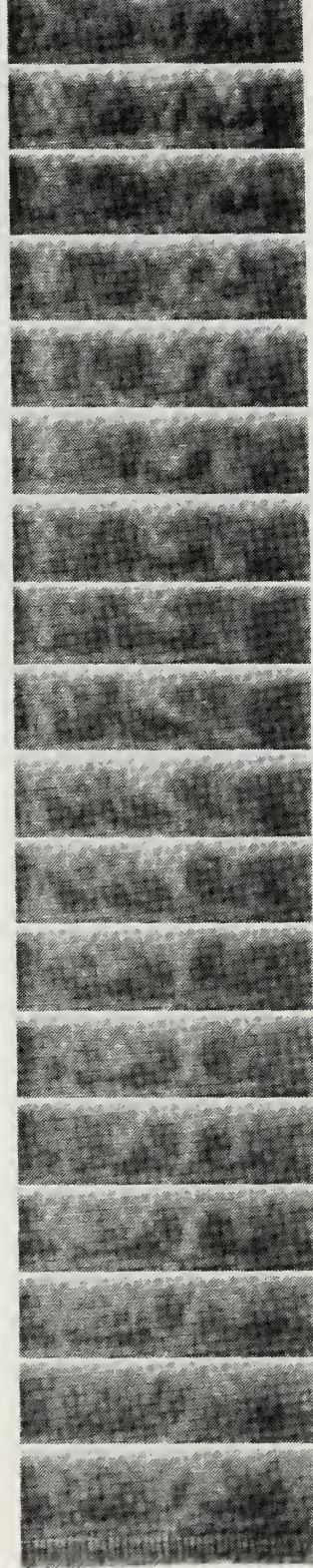


Figure 35. Flow Visualization Results $De = 100$ $\theta = 155^\circ$

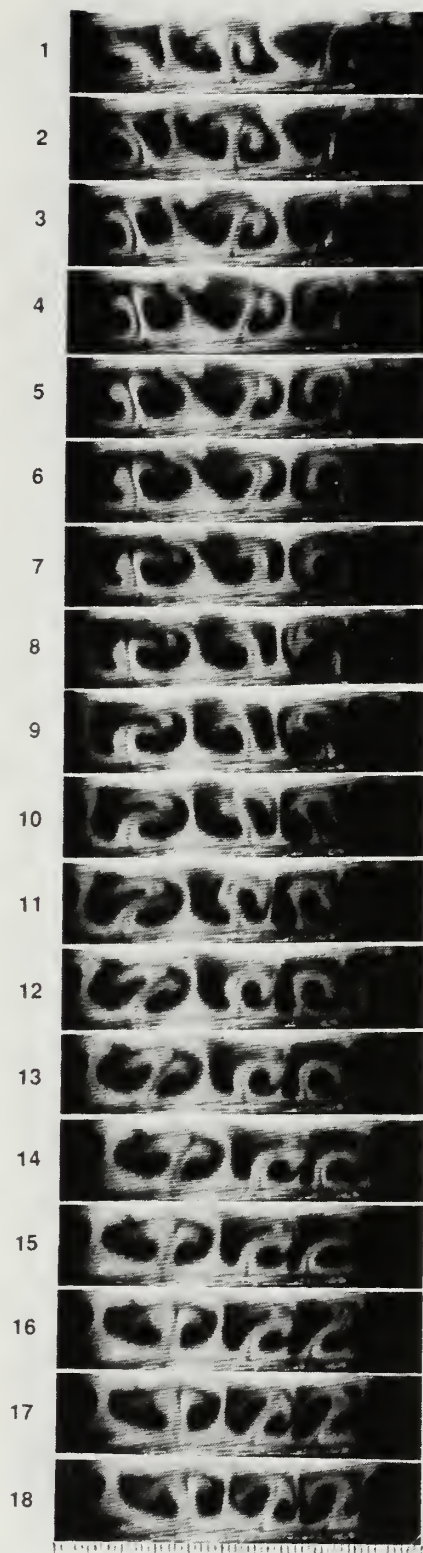


Figure 36. Flow Visualization Results $De = 125$ $\theta = 115^\circ$ (1 of 2)

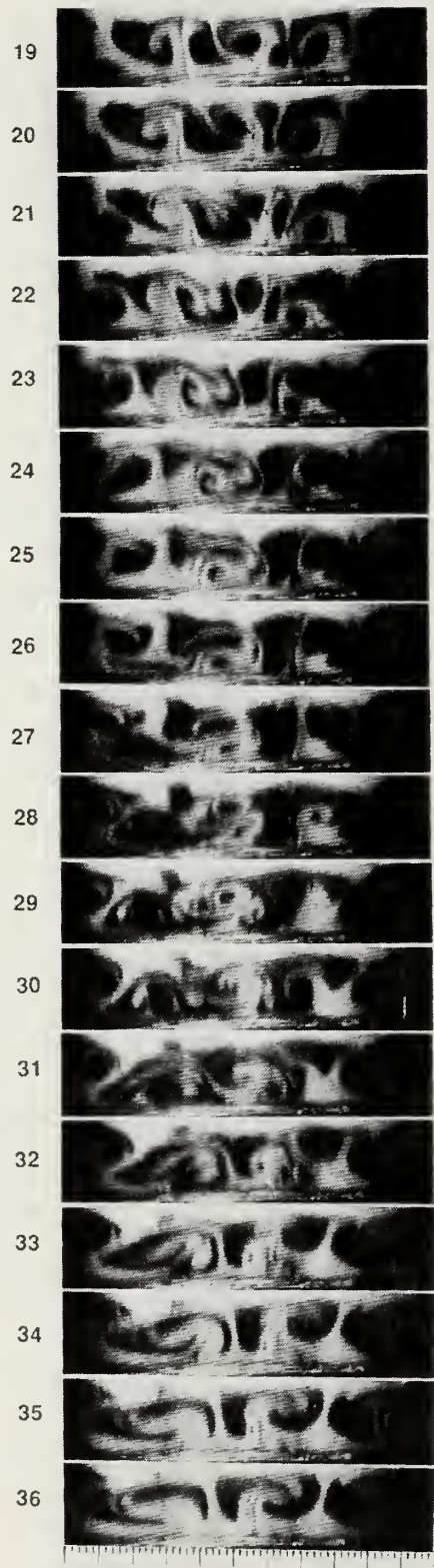


Figure 37. Flow Visualization Results $De = 125$ $\theta = 115^\circ$ (2 of 2)

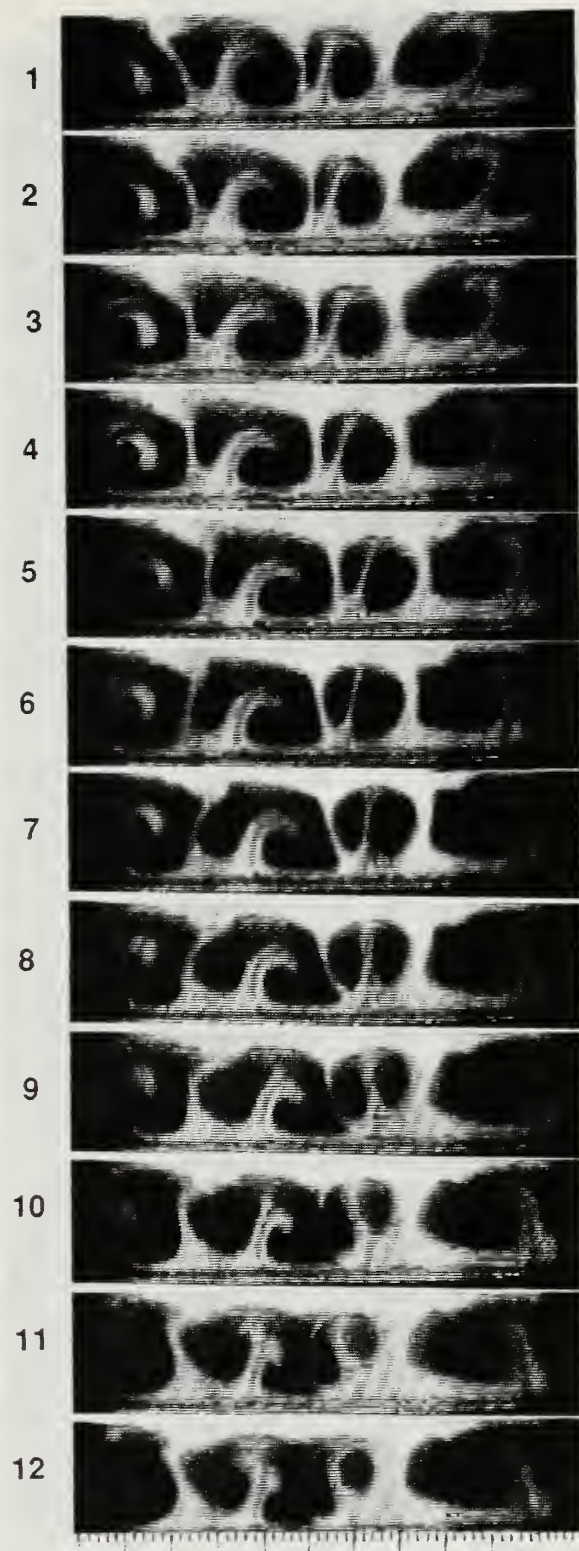


Figure 38. Flow Visualization Results $De = 100$ $\theta = 125^\circ$ (1 of 2)

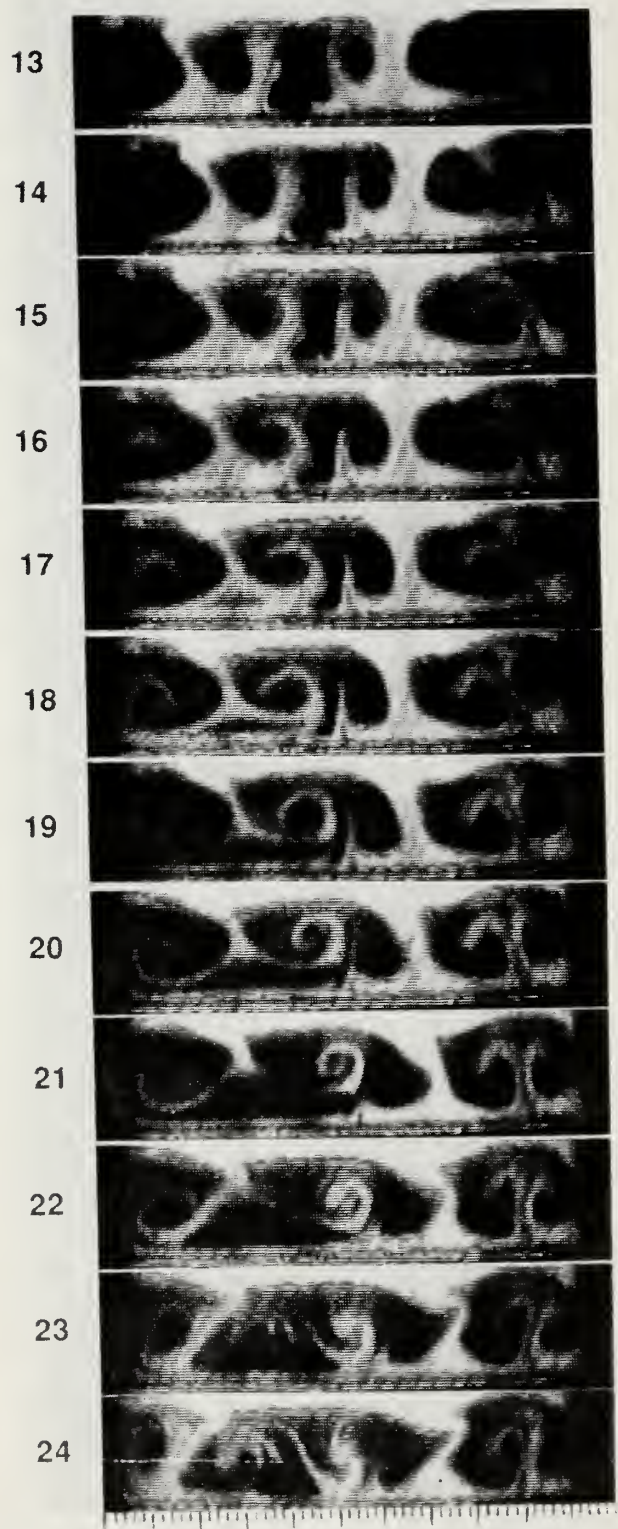


Figure 39. Flow Visualization Results $De = 100$ $\theta = 125^\circ$ (2 of 2)

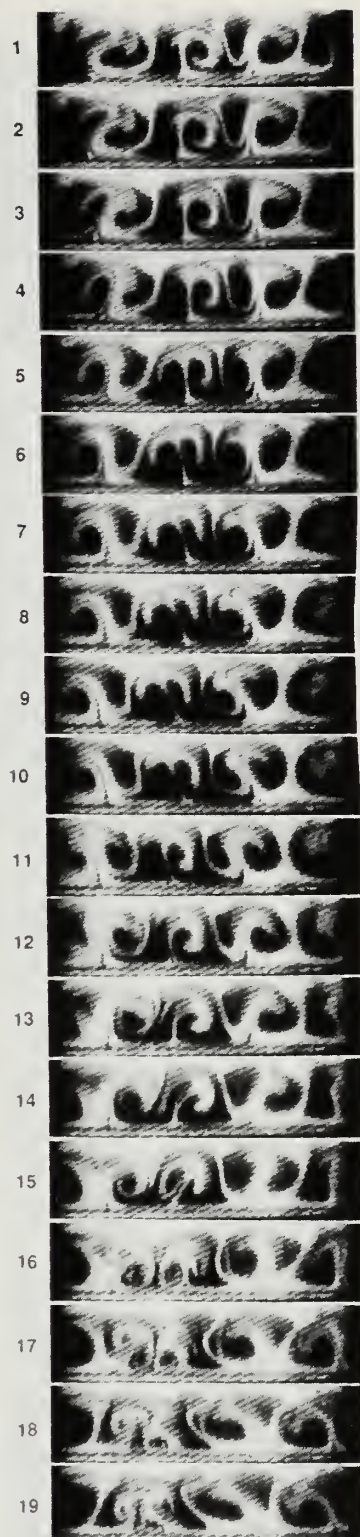


Figure 40. Flow Visualization Results $De = 100$ $\theta = 125^\circ$ (1 of 2)

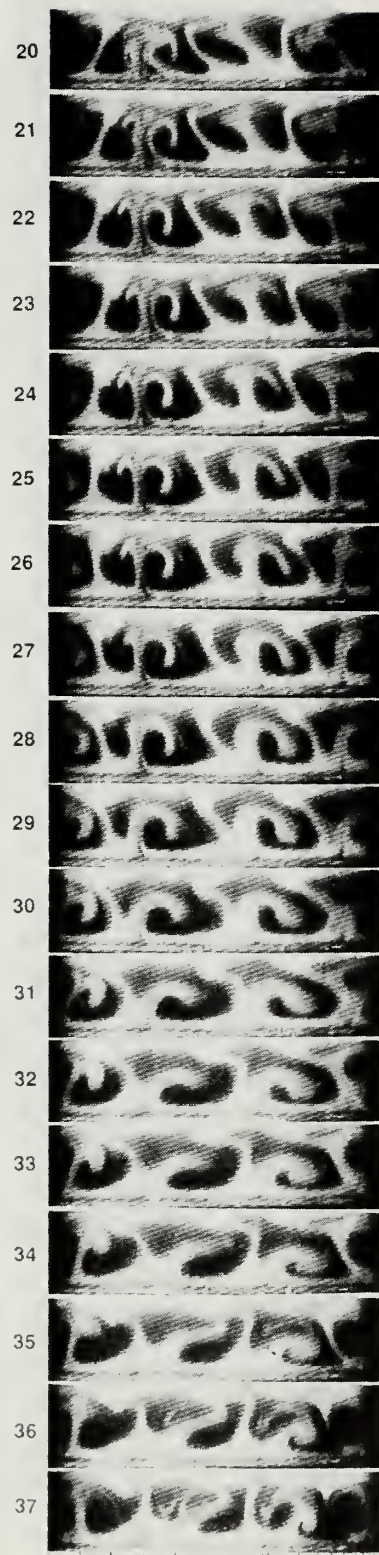


Figure 41. Flow Visualization Results $De = 100$ $\theta = 125^\circ$ (2 of 2)

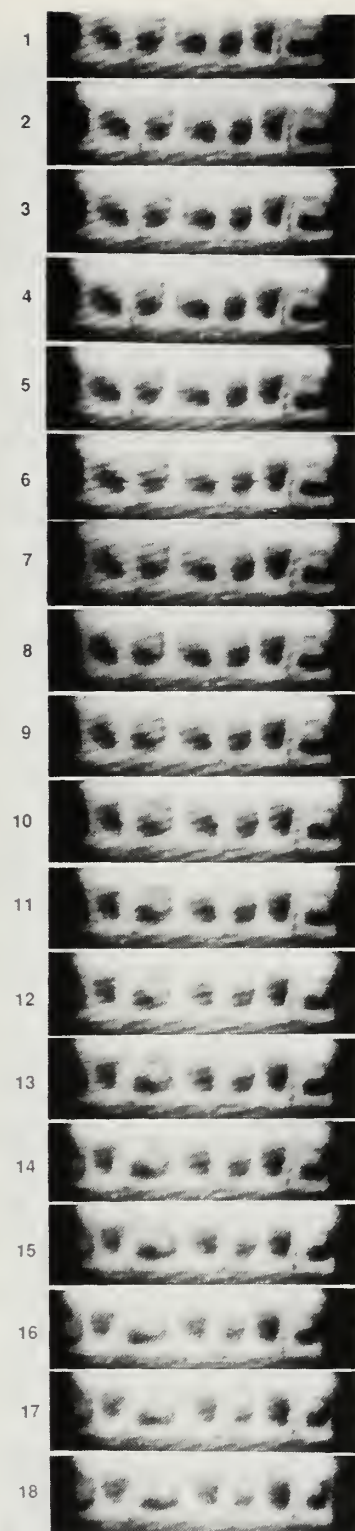


Figure 42. Flow Visualization Results $De = 75$ $\theta = 135^\circ$ (1 of 2)

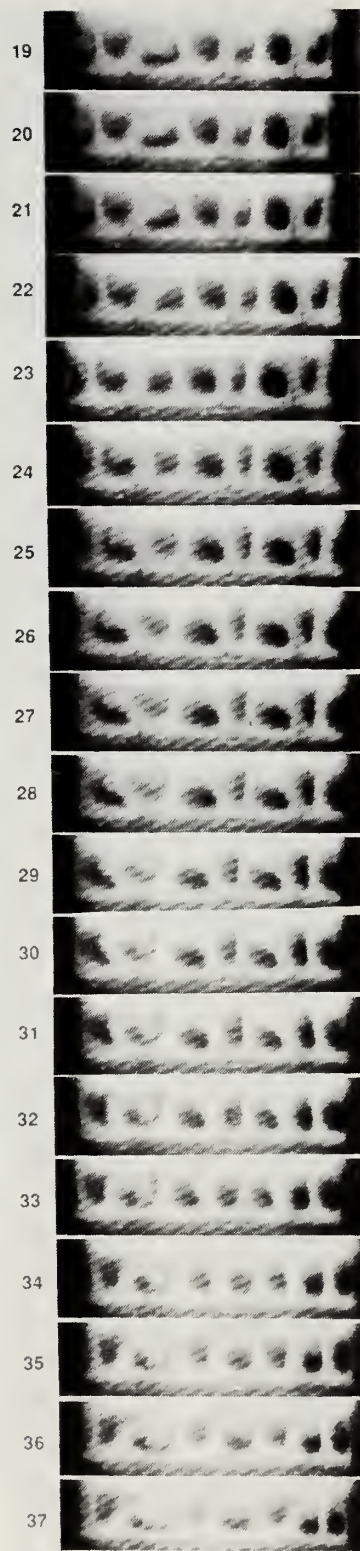


Figure 43. Flow Visualization Results $De = 75$ $\theta = 135^\circ$ (2 of 2)

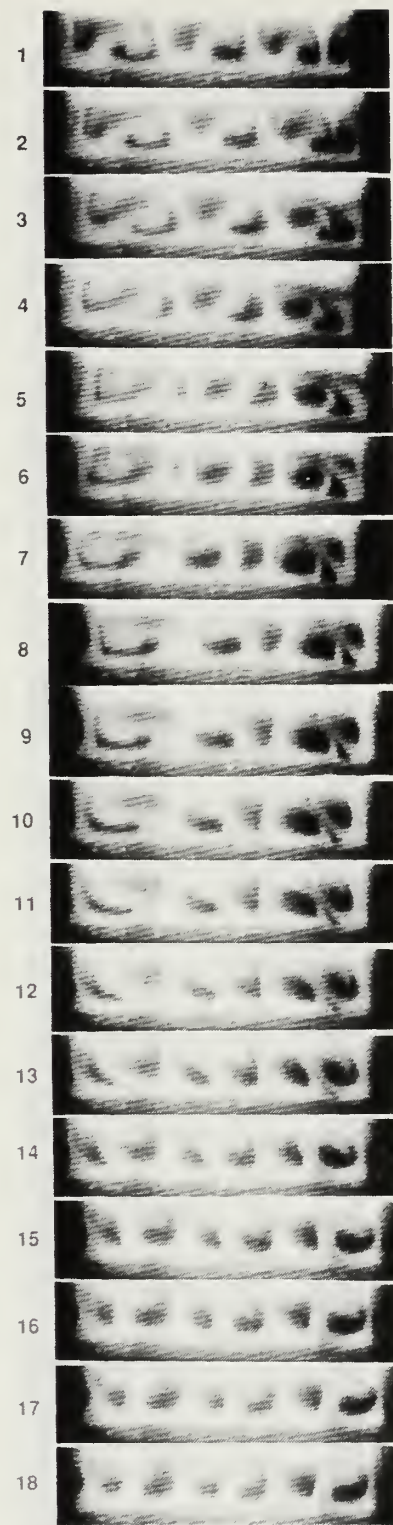


Figure 44. Flow Visualization Results $De = 75$ $\theta = 135^\circ$ (1 of 2)

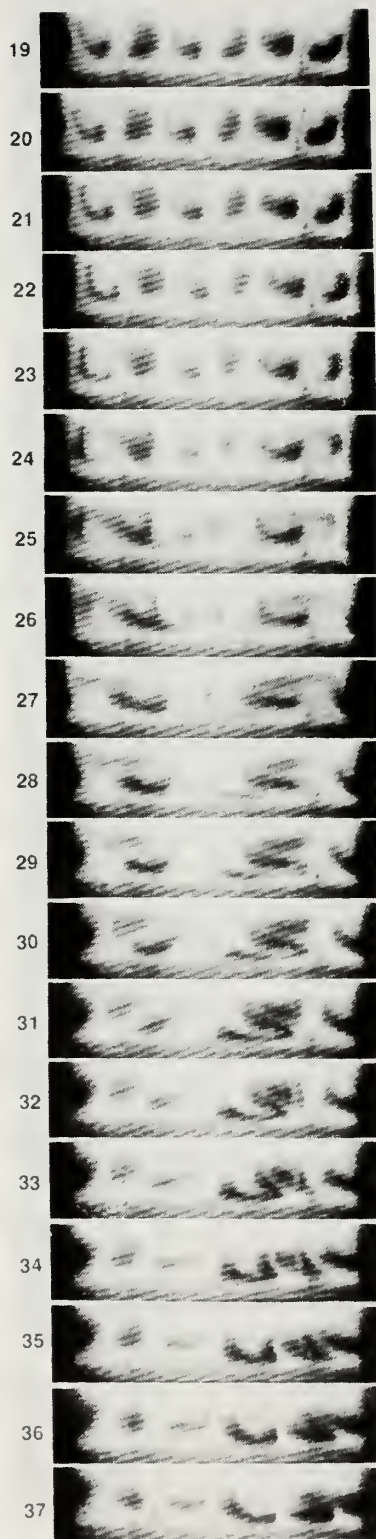


Figure 45. Flow Visualization Results $De = 75$ $\theta = 135^\circ$ (2 of 2)

RUN #50289.1759 DEAN = 50
 U_x

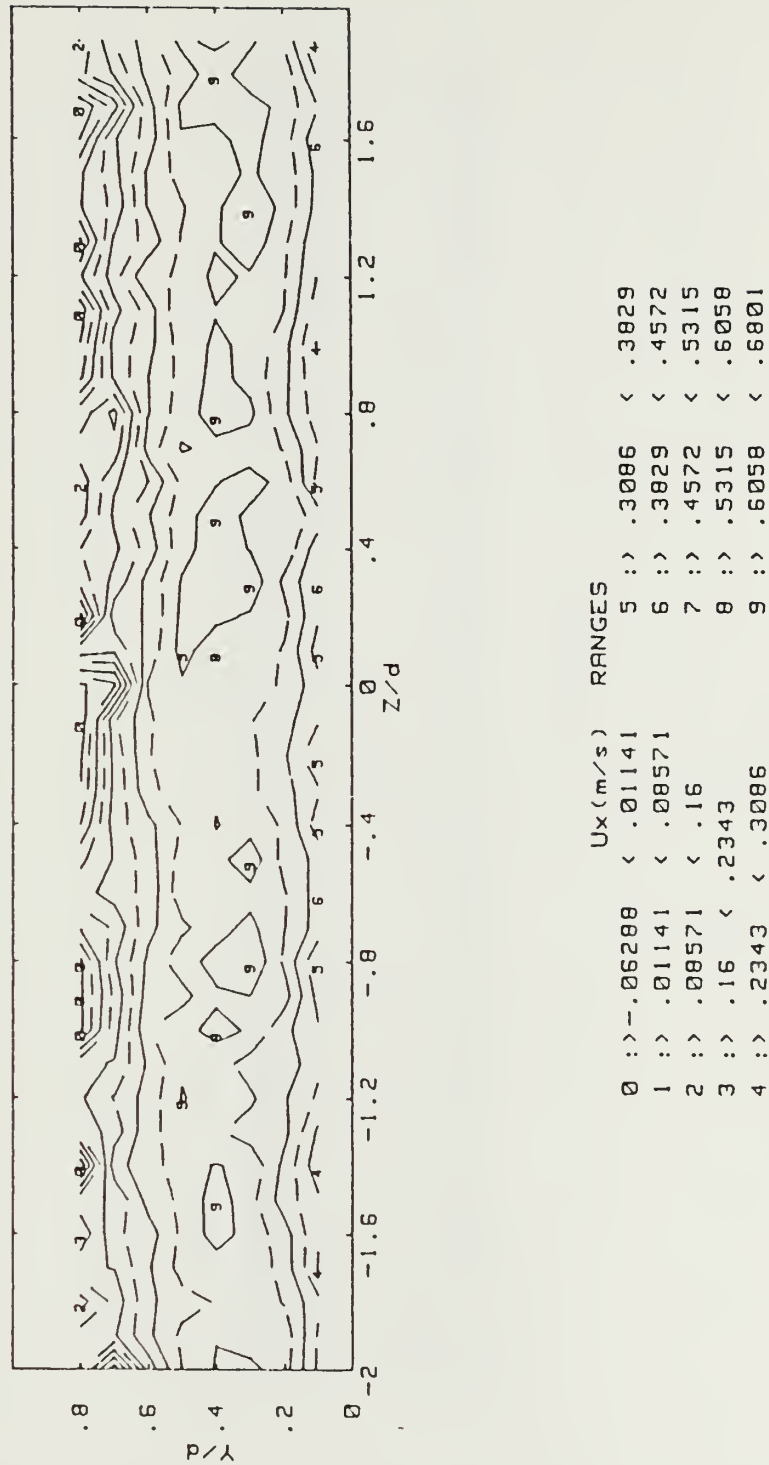
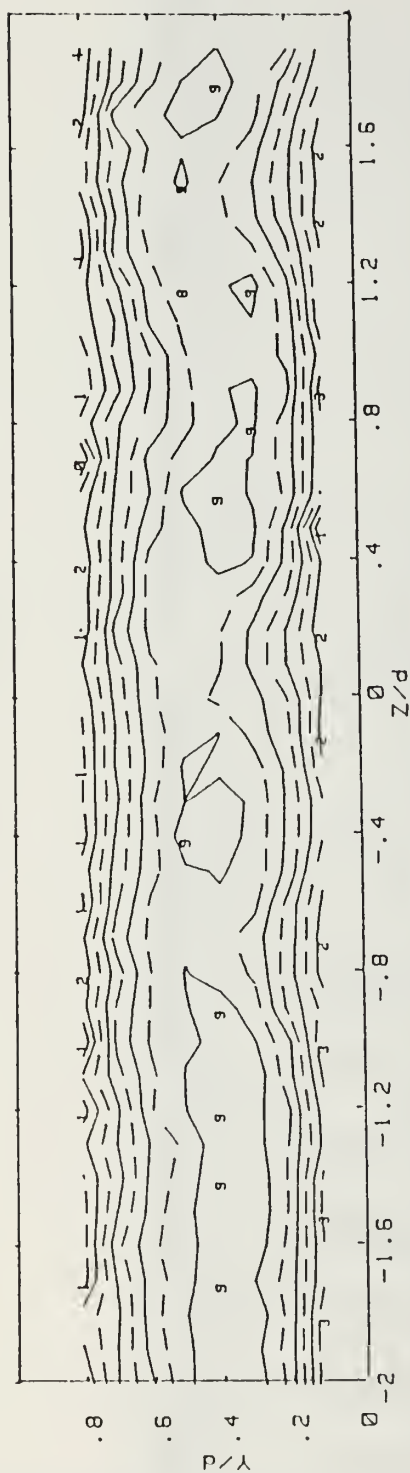


Figure 46. Streamwise Velocity Contours in a Curved Channel, $De = 50$

RUN #42989.0955 DEAN = 75

U_x



U_x (m/s)		RANGES	
0 :>	.3925	5 :>	.7493
1 :>	.4639	6 :>	.8206
2 :>	.5352	7 :>	.8919
3 :>	.6066	8 :>	.9633
4 :>	.6779	9 :>	1.035
			1.106

Figure 47. Streamwise Velocity Contours in a Curved Channel, $De = 75$

RUN #42989.2101 DEAN = 100
 U_x

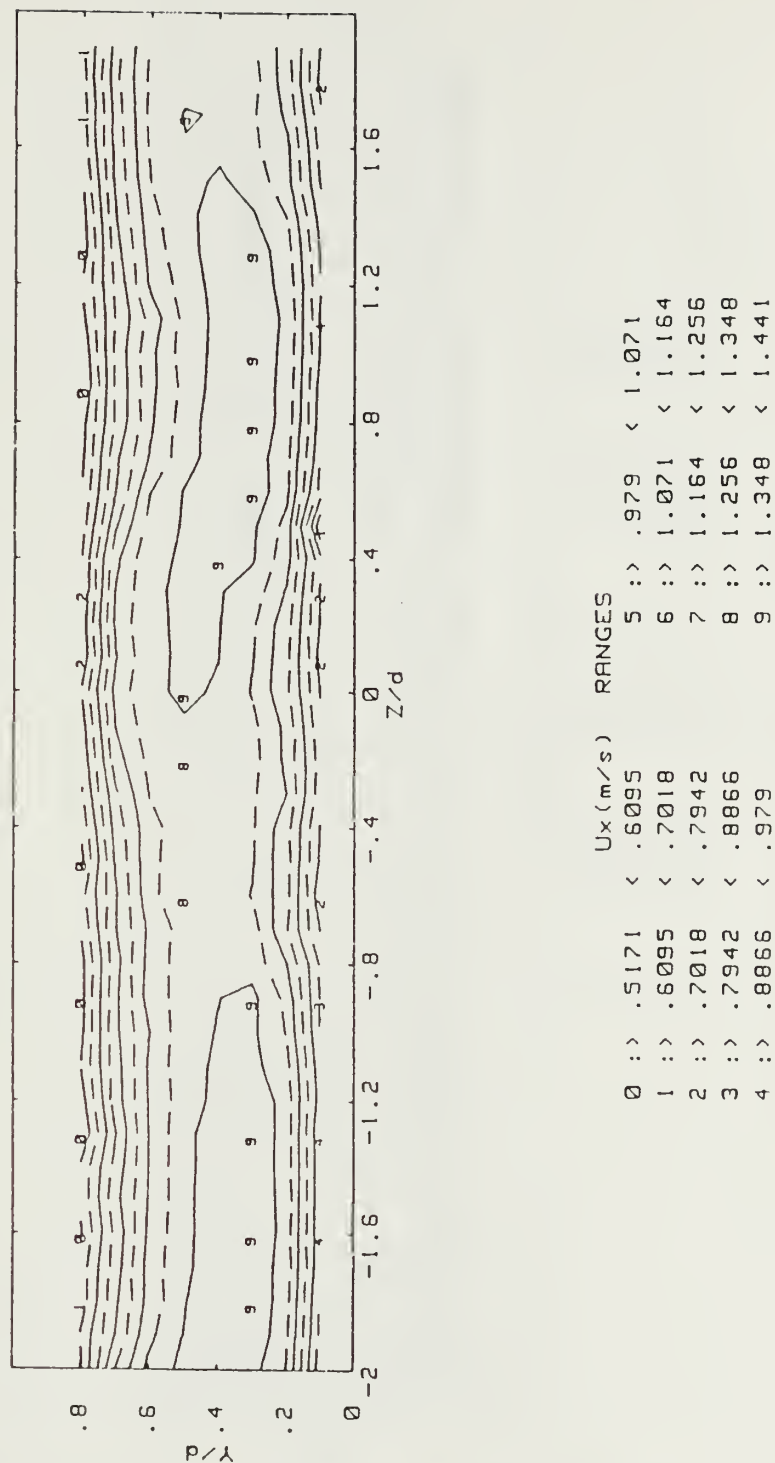


Figure 48. Streamwise Velocity Contours in a Curved Channel, $De = 100$

RUN #43089.1253 DEAN = 150
 U_x

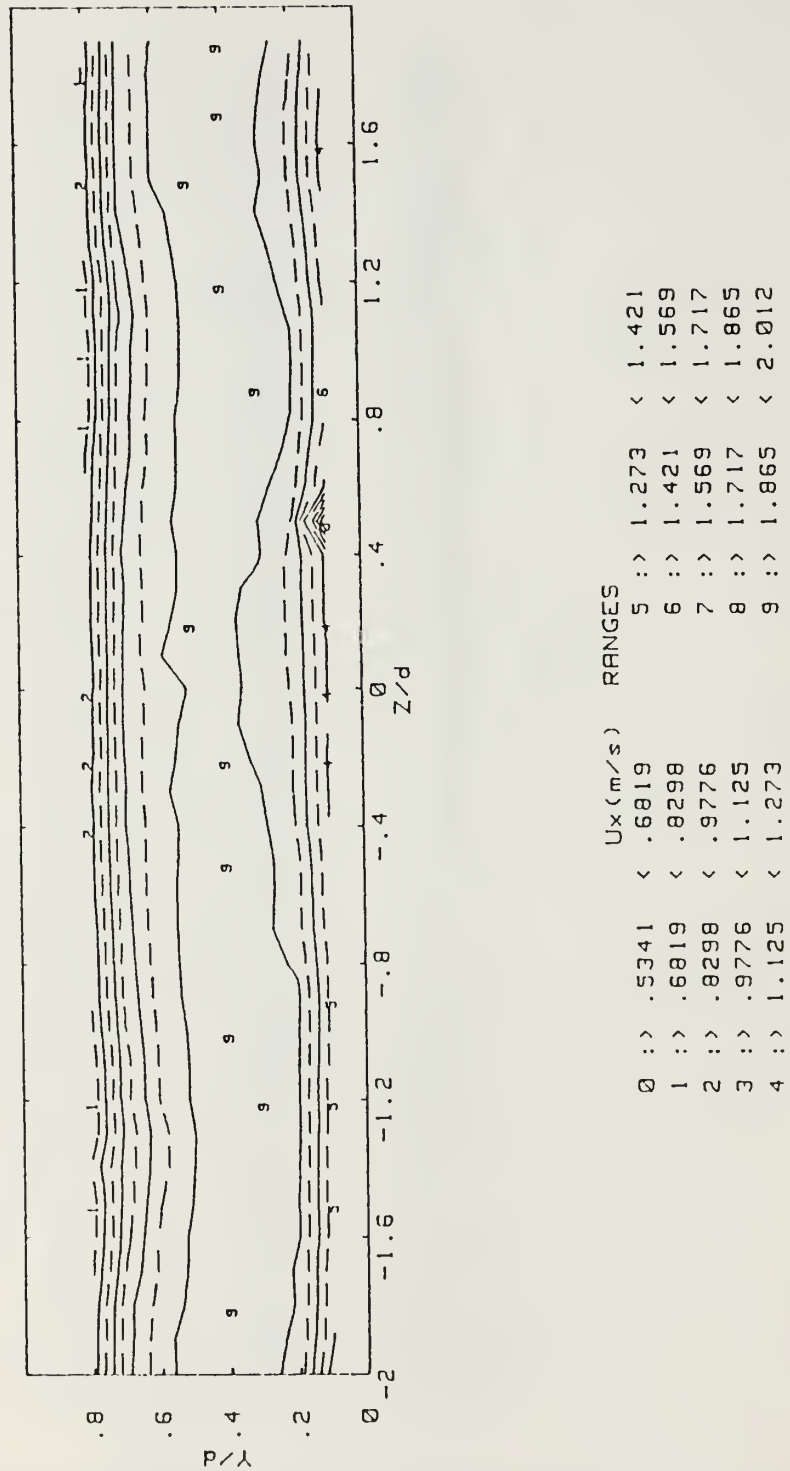


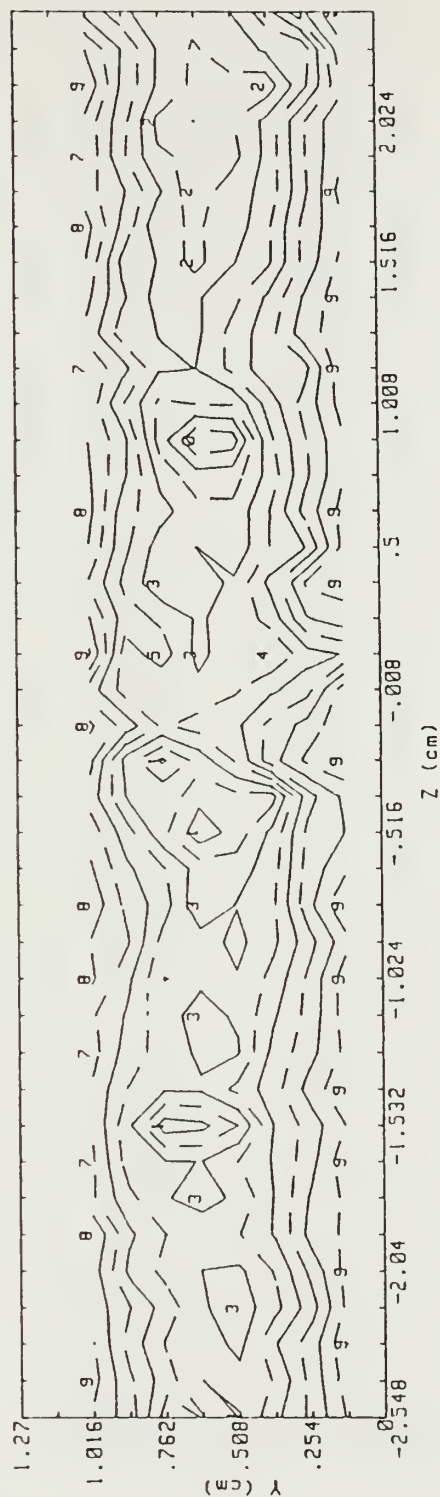
Figure 49. Streamwise Velocity Contours in a Curved Channel, $De = 150$

TOTAL PRESSURE CONTOURS CURVED CHANNEL Pamb-Pp1n (IN WATER)

AVE. DEAN = 50.0

FILES AVERAGED

41489.0915



PRESSURE RANGES	
0	.0129 .0131 5
1	.0131 .0133 6
2	.0133 .0134 7
3	.0134 .0136 8
4	.0136 .0138 9
	.0138 .0139
	.0139 .0141
	.0141 .0143
	.0143 .0145
	.0145 .0146

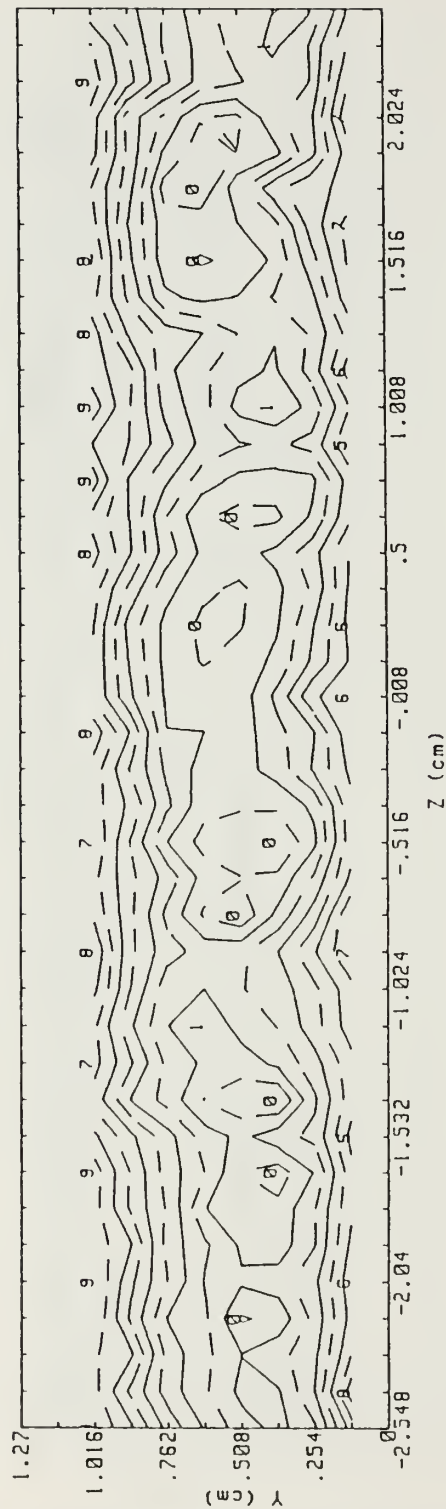
Figure 50. Total Pressure Contours in a Curved Channel, De = 50

TOTAL PRESSURE CONTOURS CURVED CHANNEL Pamb-Pp1n (IN WATER)

AVE. DEAN = 75.0

FILES AVERAGED

41489.1620



PRESSURE RANGES				
0	.0230	.0233	5	.0249
1	.0233	.0237	6	.0253
2	.0237	.0241	7	.0256
3	.0241	.0245	8	.0260
4	.0245	.0249	9	.0264
				.0268

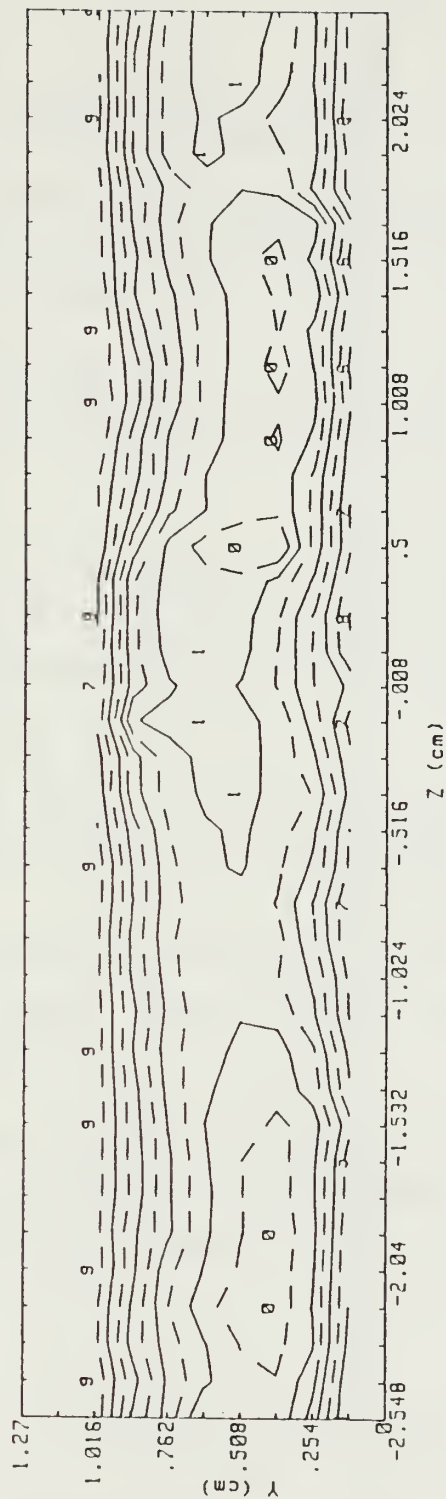
Figure 51. Total Pressure Contours in a Curved Channel, $De = 75$

TOTAL PRESSURE CONTOURS CURVED CHANNEL Pamb-Pp1n (IN WATER)

AVE. DEAN = 100.0

FILES AVERAGED

41789.1400



PRESSURE RANGES				
0	.0368	.0376	5	.0405
1	.0376	.0383	6	.0412
2	.0383	.0390	7	.0420
3	.0390	.0398	8	.0427
4	.0398	.0405	9	.0434
				.0442

Figure 52. Total Pressure Contours in a Curved Channel, $De = 100$

TOTAL PRESSURE CONTOURS CURVED CHANNEL Pamb-Pp1n (IN WATER)

AVE. DEAN = 155.55
FILES AVERAGED

41989.1630

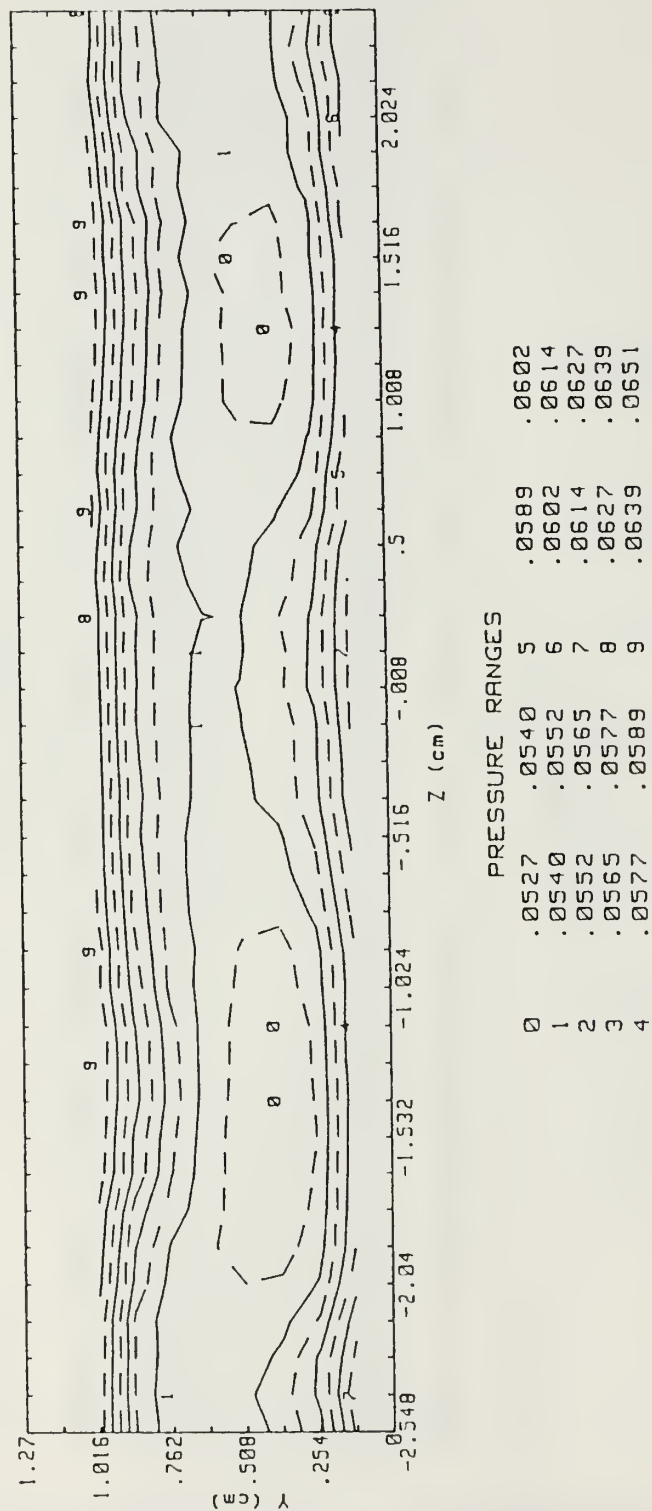


Figure 53. Total Pressure Contours in a Curved Channel, $De = 155.55$

LIST OF REFERENCES

1. Baun, L. R., *The Development and Structural Characteristics of Dean Vortices in a Curved Rectangular Channel* , Master's and Engineer's Thesis, Naval Postgraduate School, Monterey, CA., September 1988.
2. Siedband, M. A., *A Flow Visualization Study of Laminar/Turbulent Transition in a Curved Channel* , Master's Thesis, Naval Postgraduate School, Monterey, CA., March 1987.
3. Longest, J. M., *Flow Visualization Studies in (1) A Curved Rectangular Channel With 40 to 1 Aspect Ratio and (2) A Straight Channel With Imposed Bulk Flow Unsteadiness* , Master's Thesis, Naval Postgraduate School, Monterey, CA., June 1989.
4. Schwartz, G. E., *Control of Embedded Vortices Using Wall Jets* , Master's Thesis, Naval Postgraduate School, Monterey, CA., September 1988.
5. Bella, D. W., *Flow Visualization of Time-Varying Structural Characteristics of Dean Vortices in a Curved Channel* , Master's Thesis, Naval Postgraduate School, Monterey, CA., September 1988.
6. Ligrani, P.M., Singer, B.A., and Baun, L.R., "Miniature Five Hole Pressure Probe for Measurement of Three Mean Velocity Components in Low Speed Flows," submitted to *Journal of Physics E- Scientific Instruments* ,1988.

INITIAL DISTRIBUTION LIST

		No. Copies
1.	Defense Technical Information Center Cameron Station Alexandria, VA 22304-6145	2
2.	Library, Code 0142 Naval Postgraduate School Monterey, CA 93943-5002	2
3.	Professor Phillip M. Ligrani Code 069Li Naval Postgraduate School Monterey, CA 93943-5000	8
4.	Professor Chelakara S.Subramanian Code 069Su Naval Postgraduate School Monterey, CA 93943-5000	2
5.	Department Chairman, Code 69 Department of Mechanical Engineering Naval Postgraduate School Monterey, CA 93943-5000	1
6.	LT Randy E. Hughes 4613 Revere Drive Virginia Beach, VA 23456	2
7.	Dr. K. Civinskas Propulsion Directorate U.S. Army Aviation Res. and Technology Activity AVSCOM NASA-Lewis Research Center Cleveland, OH 45433	8

617-586

Thesis

H85793 Hughes

c.1 Development qualification and measurements in two curved channels with 40 to 1 aspect ratio.

Thesis

H85793 Hughes

c.1 Development qualification and measurements in two curved channels with 40 to 1 aspect ratio.



thesH85793
Development qualification and measuremen



3 2768 000 89043 8
DUDLEY KNOX LIBRARY